Cell Reports

Article

Interleukin-23 receptor signaling impairs the stability and function of colonic regulatory T cells

Graphical abstract

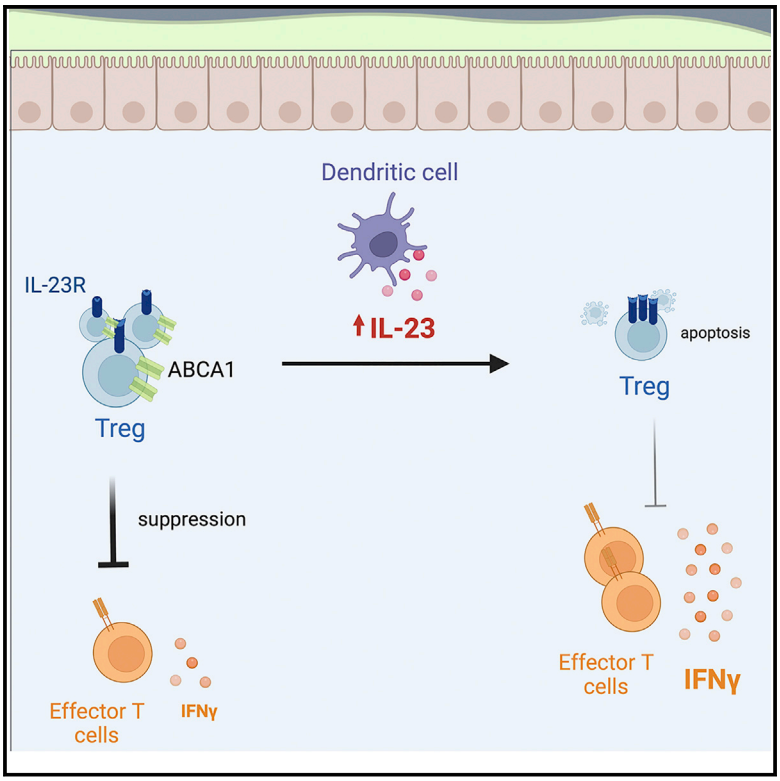

Authors

Justin Jacobse, Rachel E. Brown, Jing Li, ..., Edmond H.H.M. Rings, Janneke N. Samsom, Jeremy A. Goettel

Correspondence

jeremy.goettel@vumc.org

In brief

Jacobse et al. show the cytokine interleukin-23 specifically negatively regulates suppressive function and survival of intestinal regulatory T cells in mice.

Highlights

- Studying IL-23R signaling in Tregs requires a focus on intestinal Tregs
- IL-23R-deficient Tregs have a cell-intrinsic advantage over IL-23R-sufficient Tregs
- IL-23R-signaling increases apoptosis in intestinal Tregs
- Cholesterol homeostasis is altered in IL-23R-deficient colonic Tregs

Jacobse et al., 2023, Cell Reports *42*, 112128
February 28, 2023
https://doi.org/10.1016/j.celrep.2023.112128

CellPress

Cell Reports

CellPress
OPEN ACCESS

Article

Interleukin-23 receptor signaling impairs the stability and function of colonic regulatory T cells

Justin Jacobse,[1,2,3,4] Rachel E. Brown,[5,6] Jing Li,[3] Jennifer M. Pilat,[5] Ly Pham,[3] Sarah P. Short,[1,5,7] Christopher T. Peek,[3,6] Andrea Rolong,[8] M. Kay Washington,[3,7] Ruben Martinez-Barricarte,[3,9,10,11] Mariana X. Byndloss,[3,7,10,14] Catherine Shelton,[3] Janet G. Markle,[3,9,10,11] Yvonne L. Latour,[1,3] Margaret M. Allaman,[1] James E. Cassat,[3,7,10,12,13,14,15] Keith T. Wilson,[1,3,4,5,7,10,14] Yash A. Choksi,[1,4,5,7] Christopher S. Williams,[1,5,7] Ken S. Lau,[7,8] Charles R. Flynn,[16] Jean-Laurent Casanova,[17,18,19,20,21] Edmond H.H.M. Rings,[2,22] Janneke N. Samsom,[23] and Jeremy A. Goettel[1,3,5,7,10,24,*]

[1]Department of Medicine, Division of Gastroenterology, Hepatology and Nutrition, Vanderbilt University Medical Center, 2215 Garland Avenue, 1075J MRB IV, Nashville, TN 37232, USA
[2]Willem-Alexander Children's Hospital, Department of Pediatrics, Leiden University Medical Center, Leiden, the Netherlands
[3]Department of Pathology, Microbiology, and Immunology, Vanderbilt University Medical Center, Nashville, TN, USA
[4]Veterans Affairs Tennessee Valley Healthcare System, Nashville, TN 37212, USA
[5]Program in Cancer Biology, Vanderbilt University School of Medicine, Nashville, TN, USA
[6]Medical Scientist Training Program, Vanderbilt University School of Medicine, Nashville, TN 37232, USA
[7]Center for Mucosal Inflammation and Cancer, Vanderbilt University Medical Center, Nashville, TN, USA
[8]Department of Cell and Developmental Biology and Epithelial Biology Center, Vanderbilt University School of Medicine, Nashville, TN, USA
[9]Department of Medicine, Division of Genetic Medicine, Vanderbilt University Medical Center, Nashville, TN, USA
[10]Vanderbilt Institute for Infection, Immunology and Inflammation, Vanderbilt University Medical Center, Nashville, TN, USA
[11]Vanderbilt Genetics Institute, Vanderbilt University Medical Center, Nashville, TN, USA
[12]Department of Biomedical Engineering, Vanderbilt University, Nashville, TN, USA
[13]Department of Pediatrics, Division of Pediatric Infectious Diseases, Vanderbilt University Medical Center, Nashville, TN, USA
[14]Vanderbilt Center for Immunobiology, Vanderbilt University Medical Center, Nashville, TN, USA
[15]Vanderbilt Center for Bone Biology, Vanderbilt University Medical Center, Nashville, TN, USA
[16]Department of Surgery, Vanderbilt University Medical Center, Nashville, TN, USA
[17]St. Giles Laboratory of Human Genetics of Infectious Diseases, Rockefeller Branch, The Rockefeller University, New York, NY, USA
[18]Laboratory of Human Genetics of Infectious Diseases, Necker Branch, Institut National de la Santé et de la Recherche Médicale (INSERM) U1163, Necker Hospital for Sick Children, Paris, France
[19]The Center for Stem Cell Biology, Sloan-Kettering Institute for Cancer Research, New York, NY, USA
[20]Developmental Biology Program, Sloan-Kettering Institute for Cancer Research, 1275 York Avenue, New York, NY, USA
[21]Howard Hughes Medical Institute, New York, NY, USA
[22]Sophia Children's Hospital, Department of Pediatrics, Erasmus University, Erasmus University Medical Center, Rotterdam, the Netherlands
[23]Laboratory of Pediatrics, Division of Gastroenterology and Nutrition, Erasmus University Medical Center, Rotterdam, the Netherlands
[24]Lead contact
*Correspondence: jeremy.goettel@vumc.org
https://doi.org/10.1016/j.celrep.2023.112128

SUMMARY

The cytokine interleukin-23 (IL-23) is involved in the pathogenesis of inflammatory and autoimmune conditions including inflammatory bowel disease (IBD). *IL23R* is enriched in intestinal Tregs, yet whether IL-23 modulates intestinal Tregs remains unknown. Here, investigating IL-23R signaling in Tregs specifically, we show that colonic Tregs highly express *Il23r* compared with Tregs from other compartments and their frequency is reduced upon IL-23 administration and impairs Treg suppressive function. Similarly, colonic Treg frequency is increased in mice lacking *Il23r* specifically in Tregs and exhibits a competitive advantage over IL-23R-sufficient Tregs during inflammation. Finally, IL-23 antagonizes liver X receptor pathway, cellular cholesterol transporter *Abca1*, and increases Treg apoptosis. Our results show that IL-23R signaling regulates intestinal Tregs by increasing cell turnover, antagonizing suppression, and decreasing cholesterol efflux. These results suggest that IL-23 negatively regulates Tregs in the intestine with potential implications for promoting chronic inflammation in patients with IBD.

INTRODUCTION

Interleukin-23 (IL-23) is a cytokine that has been implicated in the development of several autoimmune and inflammatory conditions including inflammatory bowel disease (IBD), rheumatoid arthritis, psoriasis, and multiple sclerosis.[1] However, the role of IL-23 in the pathogenesis of these diseases is unclear. For IBD, genome-wide association studies (GWAS) identified variants in

the receptor for IL-23 (*IL23R*) that are associated with disease risk.[2–4] However, GWAS data do not reveal underlying immune mechanisms, and expression of *IL23R* variants associated with IBD have yet to uncover altered receptor function. Patients with complete loss-of-function mutations in *IL23R*, *IL12RB1*, or *IL12B* show susceptibility to mycobacteria due to impaired IFNγ-dependent immunity[5–7] and do not develop spontaneous intestinal inflammation. These findings demonstrate that ablation of IL-23-dependent signaling does not result in IBD in humans, but instead suggest that heightened IL-23-dependent signaling may be contributing to IBD. Consistent with this, inhibition of IL-23 by targeting the p40 subunit (shared with IL-12), via the monoclonal antibody ustekinumab in patients with moderate to severe Crohn disease (CD), improved both remission-induction and decreased relapse compared with placebo.[8] Furthermore, treatment with risankizumab-rzaa, which specifically targets the IL-23-specific p19 subunit, has shown similar efficacy as ustekinumab in trials in patients with CD.[9] While these data highlight IL-23 as a driver of IBD, the mechanisms of disease pathogenesis have not been fully elucidated. To date, much of our understanding of IL-23 has come from murine studies highlighting its role in maintaining IL-17 producing Th17 cells and IL-22 secretion by group 3 innate lymphoid cells.[10] Yet, inhibition of IL-17A or IL-17R using monoclonal antibodies (i.e., secukinumab, AMG827) failed to improve CD in clinical trials and even worsened disease.[11,12] These observations suggest that the pathogenic function of IL-23 in IBD is likely independent from its role in regulating IL-17 production by Th17 cells and highlights the need to define the cellular targets of IL-23 that contribute to the pathogenesis of IBD.

Previous studies in mice have made use of global targeting strategies of individual subunits of IL-23 (p19 and p35, respectively) or IL-23R and reported both protective or pathogenic roles for this signaling pathway depending on whether IL-23 signaling is disrupted in innate or adaptive immune cells.[13] For instance, in the adoptive transfer model of colitis (i.e., the transfer of naive T cells into lymphopenic *Rag1*$^{-/-}$ mice) intestinal inflammation is dependent on IL-23 expression by the recipient.[14] In contrast, the *Citrobacter rodentium* infectious model of colitis requires IL-23 to prevent lethality by inducing IL-22.[15] These studies emphasize the need to study the cell-specific role of IL-23R signaling in intestinal inflammation.

Regulatory T cells (Treg cells) are a phenotypically diverse immune cell subset that are pivotal in regulating effector cell responses to inflammation.[16,17] Importantly, intestinal Treg cells differ from circulating Treg cells or those in lymphoid tissues and necessitate tissue-specific characterization.[18] Previous work under homeostatic conditions shows that *Il23r* is upregulated in intestinal Treg cells expressing retinoic acid-receptor (RAR)-related orphan receptor gamma-t (RORγt) and have a highly immunosuppressive gene signature.[19,20] Consequently, monoclonal antibodies targeting IL-23, in addition to effects on Th17 cells, may also modulate activation of this pathway in intestinal Treg cells. However, the cell-specific role of IL-23R signaling in intestinal Treg cells has not been fully elucidated. Here, we investigated the cell-intrinsic role of IL-23R in intestinal Treg cells with the aim of defining the contribution of this pathway to intestinal immune homeostasis and the impact on intestinal inflammation.

RESULTS

IL-23 signaling selectively destabilizes colonic Treg cells

Treg cells are largely defined by expression of the transcription factor forkhead box P3 (FOXP3). Since identification and labeling of FOXP3 necessitates cell fixation and permeabilization, we used mice harboring a fluorescent YFP reporter combined with Cre recombinase knocked into the endogenous *Foxp3* locus 3′ of the stop sequence (*Foxp3*$^{YFP-Cre}$ mice) to permit isolation of live Treg cells for functional characterization. We first validated that YFP expression was faithful to conventional nuclear staining of FOXP3 by co-staining for FOXP3 and GFP (cross-reactive for YFP and GFP). As expected, all GFP$^+$ cells stained positive for FOXP3$^+$ (Figure S1). Since murine colonic Treg cells have been reported to highly express *Il23r*,[19] we purified live CD4$^+$FOXP3$^+$ cells via flow cytometry (FC) from the spleen, mesenteric lymph nodes (mLNs), and colonic lamina propria (cLP) of *Foxp3*$^{YFP-Cre}$ mice. *Il23r* expression was assessed in sorted cells from each compartment and Treg cells from the colonic lamina propria expressed significantly higher levels of *Il23r* compared with mLN and splenic Treg cells respectively (Figure 1A). Using an *Il23r*^{eGFP} reporter mouse,[21] we found that approximately 30% of FOXP3$^+$ Treg cells in the cLP expresses IL-23R (Figure S2A). We then determined the impact of exogenous IL-23 on Treg cell frequency in *Foxp3*$^{YFP-Cre}$ mice. Mice were injected via the intraperitoneal (i.p.) route with 500 ng recombinant IL-23 or vehicle control as depicted in Figure 1B. Treg cell frequencies in the spleen and mLN were not altered following systemic IL-23 injection, while the frequency of colonic Treg cells was significantly reduced (Figure 1C), consistent with *Il23r* expression being highly enriched on colonic Treg cells and likely to exert an effect on these cells compared with spleen or mLN Treg cells. Exogenous IL-23 had no impact on the induction of Treg cells from naive T cells *in vitro* (Figure S3A), which is also consistent with the lack of *Il23r* expression on *in vitro* induced Treg (iTreg) cells (Figure S3B) and a previous study.[22] Subsequent studies showed that IL-23 can antagonize the IL-33-mediated induction of Treg cells *in vitro*, suggesting that IL-33 induces IL-23R expression on iTreg cells.[23,24] Therefore, we examined the expression of ST2 *in vivo* and found that while 35% of cLP Treg cells expressed ST2, only a fraction of cLP Treg cells expressed both IL-23R and ST2 (Figure S2A). Furthermore, nearly all IL-23R$^+$ Treg cells in the colon were negative for the transcription factor HELIOS (Figure S2A). Previous work under homeostatic conditions shows that *Il23r* is upregulated in intestinal Treg cells expressing RORγt. Using a transgenic *Rorc*^{tdTomato} reporter developed by our group, around 50% of colonic FOXP3$^+$ Treg cells expressed RORγt that were also highly enriched for *Il23r* expression compared with RORγt^{neg} Treg cells (Figure S2B). Taken together, *Il23r* expression is enriched on colonic Treg cells and IL-23 negatively regulates Treg cell frequency specifically in the intestine.

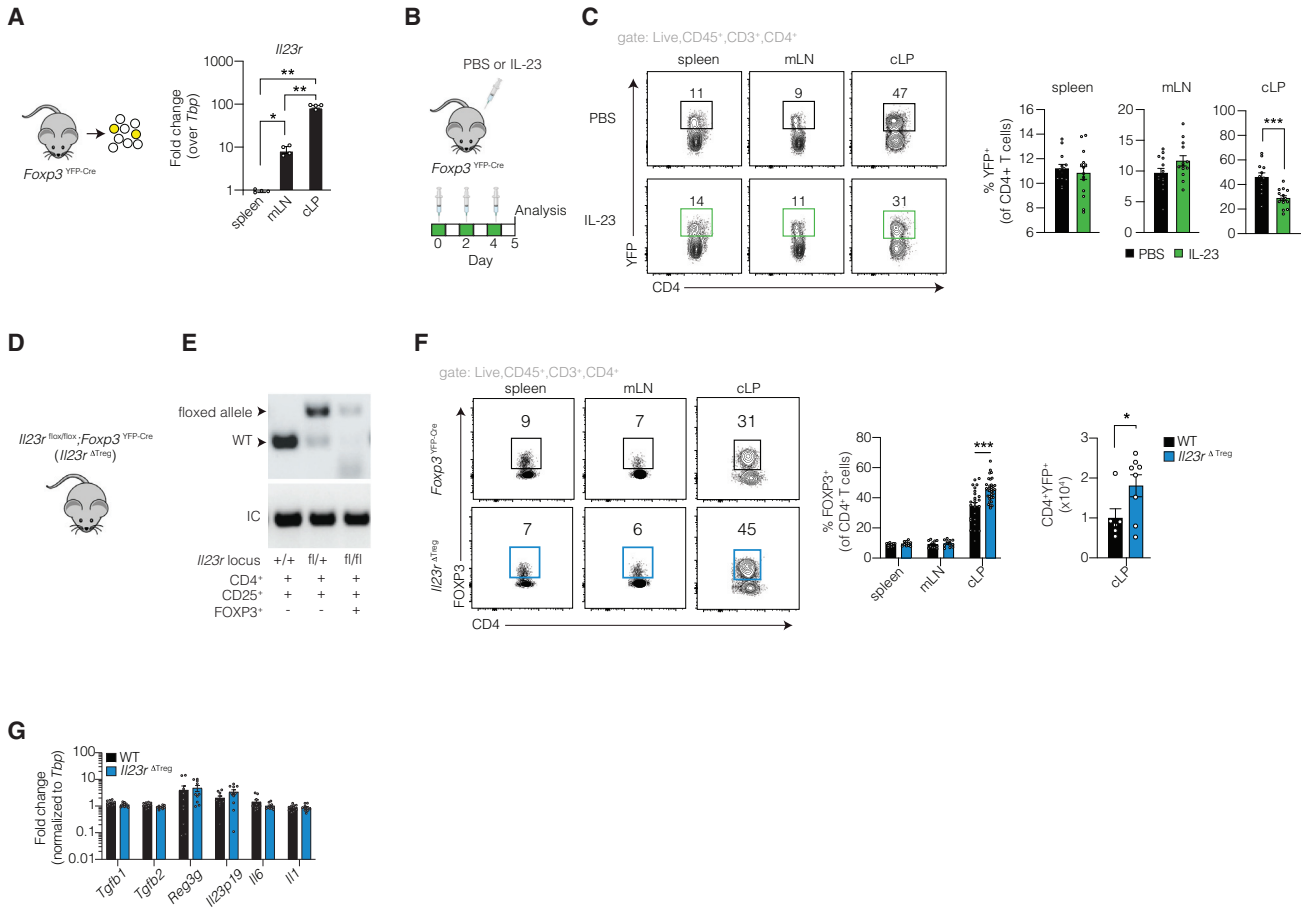

Figure 1. IL-23 negatively regulates colonic Treg cells

(A) qRT-PCR on Treg cells sorted from different compartments based on YFP for *Il23r* expression normalized to *Tbp*. Representative data of two independent experiments with n = 4.

(B) Schematic depicting *Foxp3*$^{YFP-Cre}$ mice injected with recombinant IL-23 or PBS i.p. every other day for a total of three injections.

(C) Treg cell gating and frequency quantified by flow cytometry in *Foxp3*$^{YFP-Cre}$ mice injected with IL-23 or PBS. Data are pooled from four independent experiments.

(D) *Il23r*$^{flox/flox}$*Foxp3*$^{YFP-Cre}$ (*Il23r*$^{\Delta Treg}$) mice were generated.

(E) Genotyping on DNA extracted from FACS-sorted FOXP3$^+$ cells and other CD4$^+$ T cell fractions to confirm *Il23r* deletion specific for FOXP3$^+$ cells of *Il23r*$^{\Delta Treg}$ mice. IC, internal control. Irrelevant lanes and white space were cropped.

(F) Representative FACS analysis examining Treg cell frequencies in the spleen, mLN, and colon lamina propria (cLP) of *Foxp3*$^{YFP-Cre}$ and *Il23r*$^{\Delta Treg}$ mice (left) and quantified (right) where each data point is an individual mouse. Data are pooled from more than three independent experiments.

(G) qRT-PCR of whole colon tissue RNA for genes associated with intestinal Treg induction or sustenance, normalized to *Tbp*. Histogram bars represent the mean ± SEM. (A) ANOVA with post hoc Tukey. (C, F, G) Unpaired t test. *p < 0.05, **p < 0.01, ***p < 0.001.

Cell-specific targeting of *Il23r* in FOXP3$^+$ cells increases colonic Treg cell frequency

Given our observation that exogenous IL-23 decreased colonic Treg cell frequency, we sought to determine if this effect was cell-intrinsic. To this end, we specifically targeted *Il23r* in FOXP3$^+$ Treg cells using *Il23r*$^{flox/flox}$;*Foxp3*$^{YFP-Cre}$ mice (*Il23r*$^{\Delta Treg}$ mice) (Figure 1D)[25] and confirmed selective deletion of *Il23r* in FOXP3$^+$ cells using PCR-based genotyping of sorted cell populations (Figure 1E). To determine baseline changes, we evaluated Treg cell frequency in various compartments by FC in co-housed littermates and found that *Il23r*$^{\Delta Treg}$ mice exhibited a significant increase in the frequency of Treg cells in the cLP but not in mLN or spleen that also resulted in increased absolute Treg cell numbers (Figure 1F). The increase in colonic Treg cell frequency in *Il23r*$^{\Delta Treg}$ mice was not associated with alterations in the expression of genes known to regulate intestinal Treg cells, including *Tgfb1*, *Tgfb2*, or *Il6* in whole colon tissue (Figure 1G).

Recent studies show that specific bacteria within the intestinal microbiome promote intestinal Treg cell induction via short-chain fatty acids (SCFA), a byproduct of bacterial fiber fermentation.[25–27] Therefore, we investigated whether alterations in the microbiome might explain the differences in observed Treg cell frequency in the colon of *Il23r*$^{\Delta Treg}$ mice. We performed 16S sequencing of stool DNA recovered from *Foxp3*$^{YFP-Cre}$ (wild-type [WT]) and *Il23r*$^{\Delta Treg}$ mice and detected no differences in

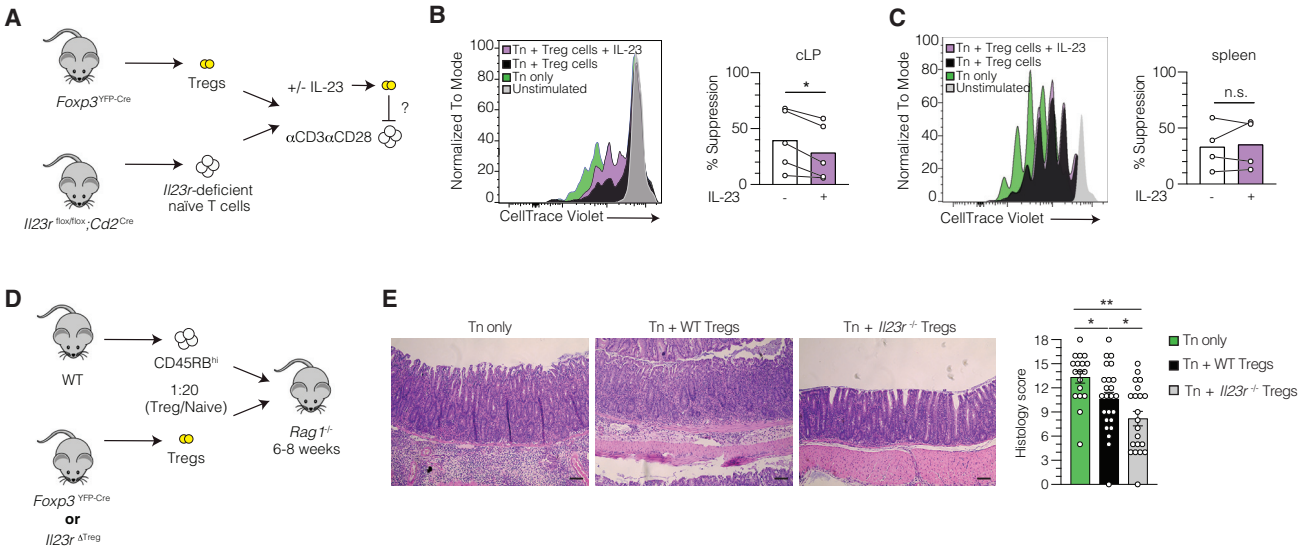

Figure 2. IL-23R signaling impairs colonic Treg cell function *in vitro* and *in vivo*

(A) Naive T cells (Tn) from spleen and mLN of a *Il23r*$^{flox/flox}$;*Cd2*^{Cre} mice were enriched by negative selection and labeled with CellTrace Violet. Tn were activated using αCD3αCD28 beads and co-cultured with sorted colonic Treg cells from *Foxp3*$^{YFP-Cre}$ mice in a 2:1 ratio Tn:Treg cells for 3 days in the presence or absence of IL-23.

(B) Representative histogram of Tn proliferation via CellTrace Violet dilution and quantification of suppression by colonic Treg cells. Data are pooled from three independent experiments. Each data point (dot) reflects cells from four or more mice and the average of two to three technical replicates.

(C) The same experiment as (B) but using Treg cells sorted from the spleen of *Foxp3*$^{YFP-Cre}$ mice.

(D) *Rag1*$^{-/-}$ mice were injected with 500,000 wild-type naive T cells with or without 25,000 Treg cells sorted from *Foxp3*$^{YFP-Cre}$ or *Il23r*$^{\Delta Treg}$ mice and euthanized between 6 and 8 weeks.

(E) Representative H&E of colon (left) and quantification of histological injury score (right). Histogram bars represent the mean ± SEM. Scale bars, 100 μm. (B and C) Paired t test. (E) Mixed-effects model with false discovery method of Benjamini, Krieger, and Yekutieli. *p < 0.05, **p < 0.01, ***p < 0.001.

beta diversity (Bray Curtis) (Figure S4A, a part of Data S1), while linear discriminant analysis (LDA) of effect size (LEFSe) indicated that *Bacilli* were more abundant in *Il23r*$^{\Delta Treg}$ mice (Figures S4B–S4D, a part of Data S1). When collapsed to the genus level, ANCOM revealed an abundance of an uncultured genus from the Ruminococcaceae family was higher in the *Il23r*$^{\Delta Treg}$ compared with the WT mice (Figures S4E, a part of Data S1). These results show that the microbiome between WT and *Il23r*$^{\Delta Treg}$ mice is highly similar but does not exclude the possibility that the small changes observed contributed to increased cLP Treg cell frequency in *Il23r*$^{\Delta Treg}$ mice. Nevertheless, broad-spectrum antibiotic treatment did not affect cLP Treg cell frequency differentially in *Il23r*$^{\Delta Treg}$ mice (Figure S4F, a part of Data S1), suggesting that the increased Treg cell frequency in *Il23r*$^{\Delta Treg}$ mice is likely independent of the microbiome. Of note, a decrease in colonic Treg cell frequency following antibiotic treatment as described by others[28] was not observed, despite a significant reduction in bacteria in the feces of antibiotic treated mice and may be attributed to vivarium conditions (data not shown).

IL-23R signaling impairs colonic Treg cell suppressive function *in vitro* and *in vivo*

With the observation that IL-23R signaling reduced intestinal Treg cell frequency, we sought to determine if there was a functional consequence in the ability of these Treg cells to regulate effector T cells. First, we performed *in vitro* suppression assays. Naive T cells were isolated from *Il23r*$^{flox/flox}$;*Cd2*^{Cre} mice (lacking IL-23R in all lymphocytes), and labeled with CellTrace Violet to track cell division. These cells were then stimulated using anti-CD3/anti-CD28 coated beads and co-cultured with sorted colonic Treg cells from *Foxp3*$^{YFP-Cre}$ mice in the presence or absence of exogenous IL-23 (Figure 2A). IL-23 impaired the suppressive function of WT Treg cells purified from the cLP *in vitro* (Figure 2B) but had no effect of on the suppressive function of Treg cells recovered from the spleen (Figure 2C), consistent with their low expression of *Il23r*. We then assessed the functional consequence of IL-23R signaling in Treg cells *in vivo.* First, we used an infectious model of colitis using *C. rodentium* that induces IL-23 production that is required for pathogen clearance.[15] *Foxp3*$^{YFP-Cre}$ and *Il23r*$^{\Delta Treg}$ mice were gavaged with a bioluminescent strain of *C. rodentium*[29] and 14 days post-infection, we observed similar colonization, colonic inflammation, and colony-forming unit (CFU) counts despite high levels of *Il23p19* transcripts (Figures S5A–S5D). These data indicate that IL-23R signaling in Treg cells does not exacerbate disease pathogenesis following infection with *C. rodentium*. We then used a second model of colitis in which IL-23 is a known driver of disease pathogenesis following the transfer of naive T cells into RAG1/2-deficient mice.[14,16,30,31] In this model, intestinal inflammation can be prevented if Treg cells are co-injected with naive T cells at a ratio of 1:5, which is sufficient to prevent exacerbated effector T cell responses.[32,33] To determine whether IL-23R-deficient Treg cells would confer enhanced suppressive function

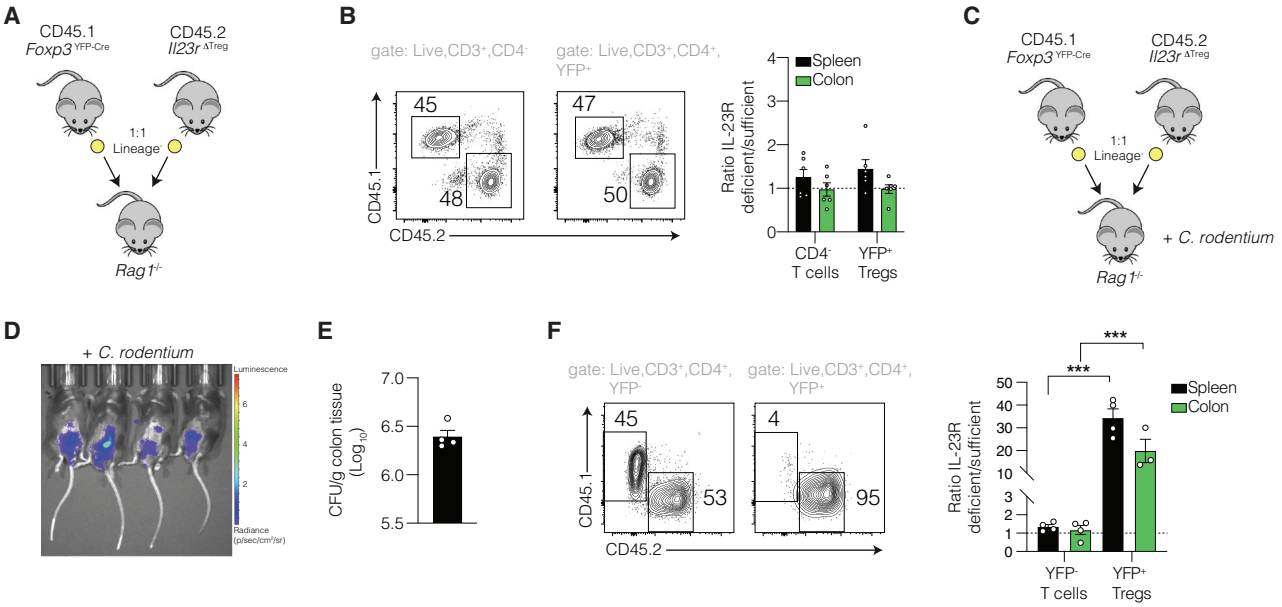

Figure 3. Selective deletion of *Il23r* in Treg cells provides a competitive advantage during *Citrobacter rodentium*-induced colitis

(A) *Rag1*$^{-/-}$ mice were sublethally irradiated (450 rads) and transplanted using a 1:1 mixture of lineage-depleted bone marrow cells from *Foxp3*$^{YFP-Cre}$CD45.1^{+} and *Il23r*$^{flox/flox}$*Foxp3*$^{YFP-Cre}$CD45.2^{+} mice.

(B) Recipient mice exhibiting a 1:1 ratio of CD4^{-} T cells were analyzed 6 to 8 weeks post-transplantation with the YFP^{+} fraction gated and the CD45.2^{+}/CD45.1^{+} ratio quantified. Data are pooled from three independent experiments.

(C) *Rag1*$^{-/-}$ were transplanted with bone marrow as in (A), 6 weeks later mice followed by gavage with *C. rodentium* (3 × 10^{8} CFU).

(D) Representative IVIS images with flux quantified for each mouse.

(E) CFU at experimental endpoint (14 days after inoculation).

(F) Flow cytometry plots of IL-23R-sufficient and IL-23R-deficient T cells (CD4^{+}FOXP3^{-}) and Treg cells (CD4^{+}FOXP3^{+}) at endpoint by flow cytometry with corresponding CD45.2/CD45.1 ratio. Histogram bars represent the mean ± SEM. (B, F) ANOVA with post hoc Tukey. ***p < 0.001.

compared to WT Treg cells, we reduced the ratio of Treg cells to naive T cells to 1:20 (Figure 2D). Compared with mice that received naive T cells alone, both mice that received IL-23R-deficient Treg cells and mice that received WT Treg cells exhibited a statistically significant improvement in disease severity based on histological analysis of hematoxylin and eosin (H&E)-stained colon sections (Figure 2E). In addition, the histology score in mice that received IL-23R-deficient Treg cells was lower compared with mice that received WT Treg cells, indicating that IL-23R-deficient Treg cells exhibit greater suppressive capacity compared with WT Treg cells. These data show that IL-23R signaling in Treg cells impairs suppressive function both *in vitro* and *in vivo*.

Survival/expansion of post-converted Treg cells is not altered by IL-23R deficiency in a transfer setting

Previous work demonstrated a requirement for IL-23R expression on naive T cells for colitis development in the adoptive T cell transfer model of colitis, suggesting that naive T cells do express IL-23R at some point to initiate disease. In this report, a slight but statistically significant increase in Treg cells converted from naive T cells was observed in recipient mice but was restricted to the colon.[22] This suggests that naive T cells do express *Il23r* and that expressions restrict colonic Treg cell induction to some extent. To address whether Treg-specific deletion of *Il23r* increased Treg cell induction or survival and/or expansion *in vivo*, we performed adoptive transfer experiments using naive T cells (CD45^{+}CD3^{+}CD4^{+}CD25^{-}CD45RB^{hi}) sorted from *Foxp3*$^{YFP-Cre}$ (WT) and *Il23r*$^{\Delta Treg}$ mice injected into *Rag1*$^{-/-}$ recipients and assessed YFP^{+} cells 6 weeks later. In this setting, we did not detect differences in Treg cell induction between groups (Figures S6A–S6C). Since this may be attributed to the microenvironment, we examined the cytokine profile in colon tissue by qPCR in established disease. The tissue profile in adoptive transfer colitis indicates a Th1 skewing in established disease based on expression of *Tbx21* and *Il12b.* whereas *Il23a* was not increased (Figure S6D). Thus, FOXP3-Cre-mediated excision of *Il23r* alleles in post-converted Treg cells appears not to impact survival or expansion in this setting.

IL-23R-deficient Treg cells exhibit a competitive advantage under inflammatory conditions

Previously, IL-23 was shown to regulate negative selection of double-positive thymocytes.[34] It is conceivable that alterations in Treg cell frequency in *Il23r*$^{\Delta Treg}$ mice could be attributed to a selective advantage of IL-23R-deficient Treg cells in a competitive setting. To investigate this, we generated mixed bone marrow chimeras in lymphocyte-deficient *Rag1*$^{-/-}$ mice. Briefly, a 1:1 ratio of lineage-depleted bone marrow progenitor cells isolated from congenically marked CD45.1;*Foxp3*$^{YFP-Cre}$ and CD45.2;*Il23r*$^{\Delta Treg}$ mice were injected retro-orbitally into sub-lethally irradiated *Rag1*$^{-/-}$ recipient mice (Figure 3A). Six to 8 weeks post-reconstitution, we

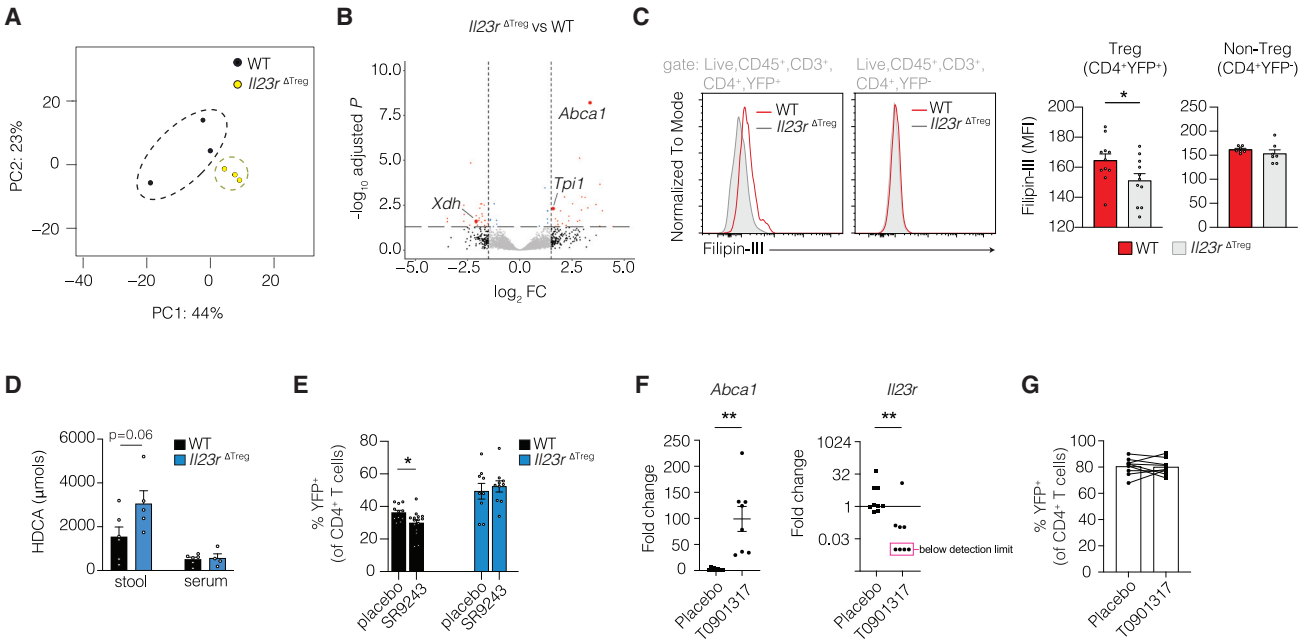

Figure 4. IL-23R-deficient colonic Treg cells exhibit altered cholesterol homeostasis

(A) RNA-sequencing was performed on FACS-sorted Treg cells (CD45$^+$CD4$^+$FOXP3$^+$ cells) from the cLP of *Foxp3*$^{YFP-Cre}$ and *Il23r*$^{\Delta Treg}$ mice with dimensionality reduction via principal-component analysis (PCA) for samples grouped based on genotype. Each dot in the PCA is representative of at least five mice.

(B) Volcano plot depicting differentially expressed genes in colonic Treg cells based on genotype.

(C) Histogram of filipin-III staining on colon YFP$^+$ or YFP$^-$ cells from *Foxp3*$^{YFP-Cre}$ and *Il23r*$^{\Delta Treg}$ mice (left) with MFI quantification (right).

(D) Secondary bile acids were quantified for stool and serum.

(E) Quantification of colonic Treg cells following treatment with vehicle control (placebo) or 30 mg kg^{-1} SR9243 for 5 days. Data are pooled from three independent experiments.

(F and G) mLN/splenic Treg cells were enriched using CD25$^+$ positive selection using magnetic beads and stimulated with αCD3αCD28 in presence of IL-2 and T0901317. After 3 days, YFP$^+$ cells were flow sorted followed by qRT-PCR for *Il23r* and *Abca1* and quantified (G). Histogram bars represent the mean ± SEM. (F and G) Data are pooled data from five independent experiments. (C, E) Unpaired t test. (F, G) Paired t test. *p < 0.05, **p < 0.01.

observed no difference in the ratio of CD45.1$^+$ and CD45.2$^+$ Treg cells in the spleen or cLP indicating that, in a competitive setting under homeostatic conditions, IL-23R-deficient Treg cells did not exhibit a selective advantage over IL-23R-sufficient Treg cells when repopulating *Rag1*$^{-/-}$ mice (Figure 3B). We then investigated whether an inflammatory setting would uncover a selective advantage, once again by inducing intestinal inflammation via infection with *C. rodentium*[33] (Figure 3C). Interestingly, although mice were equally colonized with *C. rodentium* (Figures 3D and 3E), IL-23R-deficient Treg cells comprised the majority of Treg cells in spleen and cLP 14 days post-infection, whereas the ratio of CD4$^+$Foxp3$^-$ T cells was not altered (Figure 3F). Collectively, these data indicate that under inflammatory conditions in which IL-23 is enriched, IL-23R-deficient Treg cells exhibit a competitive advantage over IL-23R-sufficient Treg cells.

IL-23R-deficient Treg cells display altered gene signatures involved in cholesterol homeostasis

In effort to define the IL-23R-dependent changes in intestinal Treg cells that might contribute to the impact on Treg cell function and selective advantage, we performed RNA-sequencing (RNA-seq) on live CD4$^+$FOXP3$^+$ cells sorted from the cLP of *Foxp3*$^{YFP-Cre}$ and *Il23r*$^{\Delta Treg}$ mice, respectively. Principal-component analysis and sample-to-sample distance indicated that Treg cells from *Foxp3*$^{YFP-Cre}$ mice and *Il23r*$^{\Delta Treg}$ mice differed (Figure 4A, a part of Data S1, GEO: GSE208621). Differential gene expression revealed 129 downregulated and 181 upregulated genes in Treg cells from *Il23r*$^{\Delta Treg}$ mice. One of the genes significantly upregulated in colonic Treg cells from *Il23r*$^{\Delta Treg}$ mice was *ATP-binding cassette a1* (*Abca1*) (Figure 4B), as were a cluster of genes associated with cell survival and liver receptor X (LXR) signaling (Figure S7). ABCA1 regulates cholesterol efflux and is the rate limiting step in high-density lipoprotein (HDL) particle assembly,[35–37] and HDL is known to increase the survival of human Treg cells.[38] To determine if increased *Abca1* altered Treg cell cholesterol content in *Il23r*$^{\Delta Treg}$ mice, we stained cells with filipin-III to detect membrane cholesterol.[39] Consistent with an increase in *Abca1* expression, colonic Treg cells from *Il23r*$^{\Delta Treg}$ mice exhibited decreased filipin-III staining compared with colonic Treg cells from WT mice (Figure 4C), suggesting that the export of cholesterol is increased in colonic IL-23R-deficient Treg cells. This is interesting, as cholesterol reduction via statins (cholesterol synthesis inhibitors) is known to increase Treg cell frequency and potentiate function.[40–42] *Abca1* expression is known to be regulated by the nuclear transcription factor LXR that can be activated by secondary bile acids such as hyodeoxycholic acid (HDCA). Therefore, we examined secondary bile acids in the serum and stool and found that HDCA was increased in the stool of *Il23r*$^{\Delta Treg}$

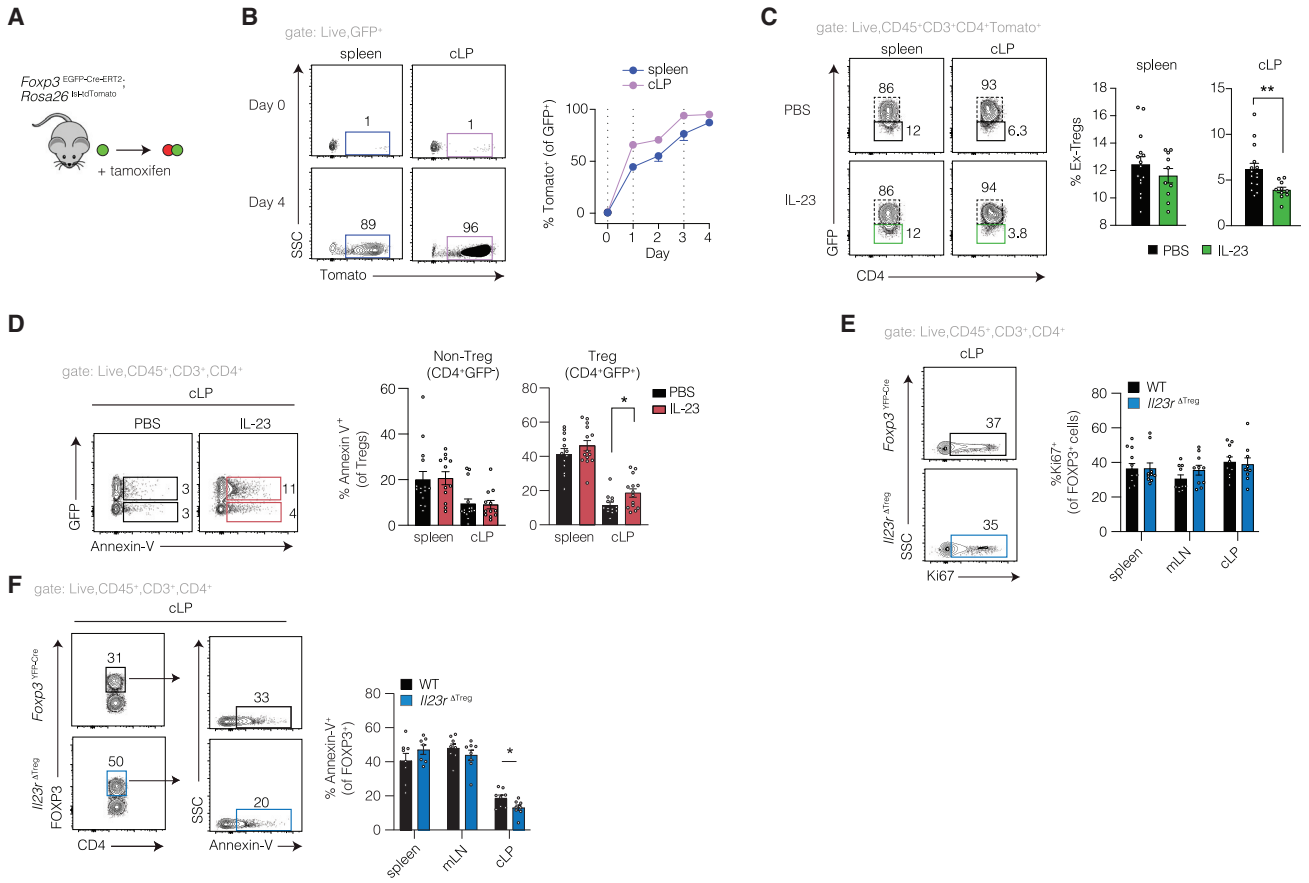

Figure 5. IL-23 reduces colonic Treg cell frequency via apoptosis

(A) Illustration of *Foxp3*$^{EGFP-Cre-ERT2}$*Rosa26*$^{lsl-tdTomato}$ mice depicting excision of the floxed stop sequence and recombination post tamoxifen. This irreversibly labels *Foxp3* expressing cells with tdTomato whereas GFP depends on continued expression of *Foxp3*.

(B) Pharmacokinetics of tamoxifen-induced recombination at the *Rosa26* locus assessed by examining tdTomato$^+$ cells among GFP$^+$ cells using flow cytometry. Representative results of two independent experiments with n = 2. Vertical dotted lines indicate tamoxifen administration.

(C) Mice were gavaged with tamoxifen and concomitantly injected with recombinant IL-23 (as for Figure 1B). Representative gating and quantification of "ex-Treg" cells; cells that are tdTomato$^+$ but GFP negative. Data are pooled from four independent experiments.

(D) Representative flow cytometry gating and quantification of Annexin-V staining. Data pooled from four independent experiments.

(E) Flow cytometry of *Foxp3*$^{YFP-Cre}$ and *Il23r*$^{\Delta Treg}$ mice at baseline for Ki67 and (F) Annexin-V. For Ki67 staining cells were fixed and permeabilized and concomitantly stained for GFP and Ki67. Histogram bars represent the mean ± SEM. (C, F) Unpaired t test. (D, E) ANOVA with post hoc Tukey. *p < 0.05, **p < 0.01.

mice compared with *Foxp3*$^{YFP-Cre}$ mice (Figure 4D). Prior work shows that treatment of mice with an LXR agonist is sufficient to increase the frequency of intestinal Treg cells[43] and partially protects from chemically induced colitis.[44] Given the upregulation of *Abca1* in IL-23R-deficient Treg cells, combined with increased HDCA in the stool, we examined whether the increased frequency of colonic Treg cells in *Il23r*$^{\Delta Treg}$ mice might require LXR signaling. To test this, *Foxp3*$^{YFP-Cre}$ mice and *Il23r*$^{\Delta Treg}$ mice were treated with an inverse agonist for LXR (SR9243) for 5 days to block LXR activation as previously described.[45] In *Foxp3*$^{YFP-Cre}$ mice, colonic Treg cell frequency was reduced following treatment with SR9243 compared with vehicle control, whereas in *Il23r*$^{\Delta Treg}$ mice, no difference in Treg cell frequency was observed (Figure 4E). Interestingly, treating Treg cells with an agonist for LXR (i.e., T0901317)[46] increased *Abca1* expression while concomitantly decreasing *Il23r* expression without impacting Treg cell stability (Figures 4F and 4G). Thus, in the setting of IL-23R deficiency, increased Treg cell frequency may indicate that while LXR activation can modulate IL-23R, the effects of IL-23R deficiency on *Abca1* is likely downstream of LXR or operating via another nuclear receptor that intersects the LXR pathway regulation.

IL-23 reduces colonic Treg cell frequency via apoptosis

Previous work established that sustained expression of FOXP3 is required for Treg cells to maintain their immunosuppressive phenotype and loss of FOXP3 expression leads to pathogenic ex-Treg cells.[47,48] Since we observed a reduction in colonic Treg cell frequency following IL-23 treatment, we sought to determine if decreased frequency was attributed to decreased FOXP3 stability. To assess this, we crossed *Foxp3*$^{EGFP-Cre-ERT2}$ mice with lineage tracing *Rosa26*$^{lox-stop-lox-tdTomato}$ mice (Figure 5A).[49] In these mice, FOXP3$^+$ cells are EGFP$^+$ (GFP$^+$) and are irreversibly labeled with tdTomato upon tamoxifen-mediated excision of the stop sequence. We first examined the pharmacokinetics of tdTomato

expression in *Foxp3*$^{EGFP-Cre-ERT2}$;*Rosa26*$^{lox-stop-lox-tdTomato}$ mice following tamoxifen administration. By day 3, the majority (>95%) of colonic Treg cells (GFP$^+$) were positive for tdTomato (Figure 5B). We then performed injections of IL-23 in these mice and observed decreased frequency of ex-Treg cells (tdTomato$^+$GFP$^-$) in the cLP but no effect was observed in the spleen (Figure 5C). This finding suggests that IL-23 does not drive conversion of Treg cells into pathogenic ex-Treg cells.

Treg cells are reported to have a relatively high turnover rate.[50] Since we observed a reduction in Treg cell frequency following IL-23 administration as well as elevated transcripts in genes associated with anti-apoptotic function in IL-23R-deficient colonic Treg cells (Figure S7), we investigated Treg cell turnover in response to exogenous IL-23. *Foxp3*$^{EGFP-Cre-ERT2}$ mice were injected with IL-23 as before and displayed an increase in Annexin-V$^+$ Treg cells that was restricted to the colon and not observed in CD4$^+$GFP$^-$ cells (Figure 5D). We then examined whether this might be a cell-intrinsic effect even in the absence of exogenous IL-23 administration at baseline. Using WT *Foxp3*$^{YFP-Cre}$ and *Il23r*$^{\Delta Treg}$ mice, we determined Treg cell proliferation using Ki67 and apoptosis via Annexin-V staining. While there were no differences in Treg cell proliferation (Figure 5E), cLP IL-23R-sufficient Treg cells exhibited a significant increase in Annexin V$^+$ cells (Figure 5F). Thus, the reduced frequency and the concomitant increased Annexin-V staining following IL-23 treatment suggest that IL-23R signaling selectively regulates colonic Treg cells, at least in part, by increasing cell turnover.

Human Treg cells within inflammatory lesions exhibit increased IL23R *expression, reduced* ABCA1*, and a pro-apoptotic gene signature*

Our observations in mice led us to explore whether Treg cells in the intestine of humans exhibit a similar phenotype in a setting in which IL-23 is present. To this end, we analyzed a single-cell RNA-seq dataset of immune cells recovered from the ileal lamina propria of patients with CD[51] (Figure S8A) and profiled a select subset of immune cells and transcripts pertaining to IL-23R and LXR signaling, and apoptosis. We found that IL-23 is expressed by inflammatory macrophages with *IL17A* expression elevated in activated conventional T cells, consistent with a role for IL-23 in stabilizing Th17 cells, and that both group 3 innate lymphoid cells and Treg cells exhibited high levels of *IL23R* expression (Figure S8B). Given the negative clinical trial data using IL-17A blockade,[11,12] we hypothesize that improvement in intestinal inflammation following administration of IL-23 blocking antibodies may be partially attributable to inhibition of IL-23R signaling in intestinal Treg cells. Consistent with our murine data, Treg cells recovered from the inflamed lesions in which IL-23 is expressed showed a slight reduction in *ABCA1* expression compared with Treg cells recovered from adjacent uninvolved intestinal tissue as well as an increase in pro-apoptotic *TNFRSF9* and *BCLAF1* (Figures S8C and S8D). Taken together, these data suggest that IL-23R signaling may function as a rheostat to modulate intestinal Treg cells in response to an IL-23-rich inflammatory environment.

DISCUSSION

Despite a clear benefit from blocking the IL-23R pathway in patients with IBD, the mechanisms and cell types through which IL-23 promotes immune dysregulation is not fully understood. Here, we showed that IL-23R signaling functions in Treg cells of the intestine and negatively regulates their frequency, function, and survival. This may explain why Treg cells present, and often increased, within inflammatory lesions are unable to exert control over effector cells leading to a chronic inflammatory state.

Similar to previous observations, we found that IL-23 did not impair TGFβ-mediated *in vitro* Treg cell induction[22] due to *in vitro* Treg cells not expressing *Il23r*. However, IL-33 has been reported to enhance the *in vitro* differentiation in Treg cells, which can be inhibited by IL-23 suggesting that IL-33 may increase *Il23r* expression during Treg cell induction *in vitro*.[23] In the intestine, most of the Treg cells are induced from naive T cells and although IL-23 is known to promote maintenance of Th17 cells, IL-17 is dispensable in a model of T cell-mediated colitis in mice.[22] Furthermore, Treg cells induced from transferred naive T cells are increased in recipient *Rag1*$^{-/-}$ mice that are unable to produce IL-23.[22] A similar observation was made if the transferred naive T cells were deficient for *Il23r*.[52] Our findings add to these data by showing that while IL-23R signaling on Treg cells impairs suppressive function, it does not impede Treg cell survival and/or expansion in the intestine since naive T cells from WT and *Il23r*$^{\Delta Treg}$ were equally competent to induce Treg cells and persist in the colons of *Rag1*$^{-/-}$ mice 6 weeks after adoptive transfer. This is intriguing, as prior work shows that Treg cells require STAT3 for suppressive function.[53] Although IL-23 induces STAT3 phosphorylation,[54] our data suggest that the negative impact of IL-23 on Treg cell function is likely not mediated by STAT3 activation.

Expression of *Il23r* in Treg cells was found to vary based on anatomic location and was largely restricted to Treg cells in the intestine where expression was highest, consistent with previous reports.[19,55] However, by directly comparing mice in which Treg cells were sufficient for IL-23R, we did find the altered Treg cell phenotype limited to the intestine. Furthermore, the impact of IL-23 on Treg suppression *in vitro* was only observed when using Treg cells recovered from the cLP, and not with Treg cells isolated from the spleen. Given the known role for IL-23 in thymic T cell selection,[34] we were surprised that IL-23R-deficient Treg cells did not have an advantage over WT Treg cells in a competitive setting at baseline. Yet, these findings align with previous data that did not identify a defect in IL-23R-deficient T cells to accumulate in the colon in other models of intestinal inflammation.[52,56,57] However, under inflammatory conditions where IL-23 is upregulated, IL-23R-deficient Treg cells were found to comprise most of the Treg cell pool at the experimental endpoint. It is tempting to speculate that cell-specific targeting of IL-23R within inflammatory settings would enable their persistence and reestablish control over effector cell responses.

Unexpectedly, we found genes associated with cell survival, LXR signaling, and *Abca1* to be upregulated in intestinal Treg cells in the absence of IL-23R. The acceptor of phospholipids and cholesterol exported by *Abca1* is apolipoprotein A1 to form HDL[58] that is then transported back to the liver via the blood as part of reverse cholesterol transport.[59] Interestingly, increased apolipoprotein A1 is also associated with an increase in Treg cells.[60] *Abca1* itself is induced by LXR activation that also

simultaneously downregulated *Il23r* expression. Unpublished findings in our lab using immortalized human B cells suggests that IL-23R signaling negatively regulates *LXR* expression, highlighting potential cross-regulation of these two pathways. Nevertheless, these data need to be confirmed in human primary Treg cells recovered from the intestine. This balance between nuclear receptor activation and IL-23R may be one way in which Treg cells in the intestine are regulated. This is similar to data in neutrophils whereby LXR activation represses IL-23R signaling.[61] The regulation of intestinal Treg cells by IL-23R signaling would fit with our observation that exogenous IL-23 increased Annexin-V staining specifically on colonic Treg cells and decreased the frequency of ex-Treg cells. While this finding seems somewhat counterintuitive, our data suggest that exogenous IL-23 promotes colonic Treg cell apoptosis and consequently, these cells are no longer a part of the colonic Treg cell pool. A similar observation was made in macrophages whereby activation of LXR also promoted cell survival.[62] Interestingly, when we sorted colonic Treg cells and cultured them *ex vivo* in the presence of IL-23, we did not observe a decrease in Treg cell frequency. Perhaps this is due to the intestinal milieu not being fully reflected *in vitro* and it is tempting to speculate that signals from macrophages or dendritic cells, major producers of IL-23, provide additional cues required to drive apoptosis in colonic Treg cells. While bacterial fermentation products such as SCFA are known to promote Treg cell induction in the intestine, it is possible that these induced Treg cells activate LXR in response to secondary bile acids to promote Treg cell maintenance by directly regulating IL-23R expression. Our group is actively investigating whether secondary bile acids modulate sensitivity to IL-23.

Altogether, we have identified a role for IL-23R signaling specifically in intestinal Treg cells that may act as a rheostat to fine-tune Treg cell function during acute inflammation, temporarily limiting suppressive capacity to allow for adequate effector cell responses. However, in settings of excessive IL-23 such as IBD, decreased Treg cell function would contribute to immune dysregulation and chronic inflammation. Defining the precise cellular mechanisms by which IL-23R antagonizes immunosuppressive programs, or possibly targeting LXR activation specifically in Treg cells to downregulate *IL23R*, has the potential to limit effector cell responses in settings of inflammation to induce remission and restore immune homeostasis.

Limitations of the study

Our study does have a few limitations. For instance, in the bone marrow chimeras, the experiments did not include a cohort of mice that received both CD45.1 and CD45.2 WT bone marrow. While this important control would detect skewing of congenic donor cells, our readout using non-$CD4^+$ T cells as an internal control did show similar reconstitution in a compartment that should be independent of FOXP3-Cre expressing cells. Another limitation is the decrease in colonic Treg cells after administration of an inverse agonist for LXR being smaller than the decrease in colonic Treg cell frequency in absence of IL-23R-signaling, indicating that other mechanisms independent of LXR may contribute or that LXR was incompletely blocked. In addition, while the results of the adoptive transfer colitis show a subtle increase in suppression of colitis by IL-23R-deficient Treg cells compared with IL-23R-sufficient Treg cells, additional factors may limit suppressive function of Treg cells, or that IL-23 indirectly affects Treg cell suppression by rendering non-Treg cells resistant to suppression. Indeed, Treg cells are not the only cell type in the intestine that expresses *Il23r*. Group 3 innate lymphoid cells are known to produce IL-22 in response to IL-23 and are key regulators of intestinal immunity.[63,64] Thus, studying whether nuclear receptor signaling in cell types including ILC3s is of considerable interest.

STAR★METHODS

Detailed methods are provided in the online version of this paper and include the following:

- KEY RESOURCES TABLE
- RESOURCE AVAILABILITY
  - Lead contact
  - Materials availability
  - Data and code availability
- EXPERIMENTAL MODEL AND SUBJECT DETAILS
  - Mice
- METHOD DETAILS
  - Colonic lamina propria
  - Adoptive transfer colitis and *in vivo* Treg cell induction
  - *In vitro* Treg cell suppression
  - Histology
  - *In vitro* Treg cell induction
  - Mixed bone marrow chimeras
  - Liver X receptor
  - Antibiotic treatment
  - RNA isolation
  - Quantitative RT-PCR (qRT-PCR)
  - RNA-sequencing
  - 16S sequencing
  - Flow cytometry
  - Bile acid analysis
- QUANTIFICATION AND STATISTICAL ANALYSIS

SUPPLEMENTAL INFORMATION

Supplemental information can be found online at https://doi.org/10.1016/j.celrep.2023.112128.

ACKNOWLEDGMENTS

Il23r floxed mice were kindly provided by Philip Rosenstiel. *C. rodentium* was a gift from Gad Frankel. Joseph Choe for technical support. Danyvid Olivares-Villagomez, Kristen Hoek, Rene Toes, and Frits Koning for critical data and manuscript discussions. The Vanderbilt Flow Cytometry Shared Resource, The Translational Pathology Shared Resource, Division of Animal Care, Center for Small Animal Imaging, and Vanderbilt Technologies for Advanced Genomics (VANTAGE) core facilities. RNA-sequencing analysis was conducted in part using the resources of the Advanced Computing Center for Research and Education at Vanderbilt University.

This work was supported by pilot grants from the Vanderbilt Digestive Disease Research Center (P30DK058404) and Vanderbilt Institute for Infection, Immunology, & Inflammation (to J.A.G.). The National Institute of Diabetes and Digestive and Kidney Diseases R03DK123489 (to J.A.G.). The Academy Ter Meulen Grant from the Royal Netherlands Academy of Arts and Sciences

and the Cultural Foundation Grant from Prince Bernhard Cultural Foundation (to J.J.). The RNA-sequencing of B cells specifically was supported by CTSA award No. UL1 TR002243 from the National Center for Advancing Translational Sciences; its contents are solely the responsibility of the authors and do not necessarily represent official views of the National Center for Advancing Translational Sciences or the National Institutes of Health. R01DK103831 to K.S.L. and P50CA236733 to A.R.

AUTHOR CONTRIBUTIONS

Conception: J.A.G. Experimental design: J.A.G., J.N.S., J.J. Experimentation: J.J., R.B., J.L., J.A.G., L.P., C.P., J.P., S.P.S. Intellectual contribution: all authors. Histopathological assessment: M.K.W. Single-cell RNA-seq analysis: A.R. and K.S.L. RNA-seq analysis: J.J., R.F., and J.A.G. Writing of manuscript: J.J. and J.A.G. Critical revision of manuscript: all authors.

DECLARATION OF INTERESTS

The authors declare no competing interests.

Received: July 21, 2022
Revised: December 29, 2022
Accepted: January 31, 2023
Published: February 17, 2023

REFERENCES

1. Croxford, A.L., Mair, F., and Becher, B. (2012). IL-23: one cytokine in control of autoimmunity. Eur. J. Immunol. *42*, 2263–2273. https://doi.org/10.1002/eji.201242598.
2. Duerr, R.H., Taylor, K.D., Brant, S.R., Rioux, J.D., Silverberg, M.S., Daly, M.J., Steinhart, A.H., Abraham, C., Regueiro, M., Griffiths, A., et al. (2006). A genome-wide association study identifies IL23R as an inflammatory bowel disease gene. Science *314*, 1461–1463. https://doi.org/10.1126/science.1135245.
3. Silverberg, M.S., Cho, J.H., Rioux, J.D., McGovern, D.P.B., Wu, J., Annese, V., Achkar, J.-P., Goyette, P., Scott, R., Xu, W., et al. (2009). Ulcerative colitis–risk loci on chromosomes 1p36 and 12q15 found by genome-wide association study. Nat. Genet. *41*, 216–220. https://doi.org/10.1038/ng.275.
4. Beaudoin, M., Goyette, P., Boucher, G., Lo, K.S., Rivas, M.A., Stevens, C., Alikashani, A., Ladouceur, M., Ellinghaus, D., Törkvist, L., et al. (2013). Deep resequencing of GWAS loci identifies rare variants in CARD9, IL23R and RNF186 that are associated with ulcerative colitis. PLoS Genet. *9*, e1003723. https://doi.org/10.1371/journal.pgen.1003723.
5. Martínez-Barricarte, R., Markle, J.G., Ma, C.S., Deenick, E.K., Ramírez-Alejo, N., Mele, F., Latorre, D., Mahdaviani, S.A., Aytekin, C., Mansouri, D., et al. (2018). Human IFN-γ immunity to mycobacteria is governed by both IL-12 and IL-23. Sci. Immunol. *3*, eaau6759. https://doi.org/10.1126/sciimmunol.aau6759.
6. Picard, C., Fieschi, C., Altare, F., Al-Jumaah, S., Al-Hajjar, S., Feinberg, J., Dupuis, S., Soudais, C., Al-Mohsen, I.Z., Génin, E., et al. (2002). Inherited interleukin-12 deficiency: IL12B genotype and clinical phenotype of 13 patients from six kindreds. Am. J. Hum. Genet. *70*, 336–348. https://doi.org/10.1086/338625.
7. de Beaucoudrey, L., Puel, A., Filipe-Santos, O., Cobat, A., Ghandil, P., Chrabieh, M., Feinberg, J., von Bernuth, H., Samarina, A., Jannière, L., et al. (2008). Mutations in STAT3 and IL12RB1 impair the development of human IL-17-producing T cells. J. Exp. Med. *205*, 1543–1550. https://doi.org/10.1084/jem.20080321.
8. Kotze, P.G., Ma, C., Almutairdi, A., and Panaccione, R. (2018). Clinical utility of ustekinumab in crohn's disease. J. Inflamm. Res. *11*, 35–47. https://doi.org/10.2147/JIR.S157358.
9. D'Haens, G., Panaccione, R., Baert, F., Bossuyt, P., Colombel, J.F., Danese, S., Dubinsky, M., Feagan, B.G., Hisamatsu, T., Lim, A., et al. (2022). Risankizumab as induction therapy for Crohn's disease: results from the phase 3 ADVANCE and MOTIVATE induction trials. Lancet *399*, 2015–2030. https://doi.org/10.1016/S0140-6736(22)00467-6.
10. Gaffen, S.L., Jain, R., Garg, A.v., and Cua, D.J. (2014). IL-23-IL-17 immune axis: discovery, mechanistic understanding, and clinical testing. Nat. Rev. Immunol. *14*, 585–600. https://doi.org/10.1038/NRI3707.
11. Targan, S.R., Feagan, B.G., Vermeire, S., Panaccione, R., Melmed, G.Y., Blosch, C., Newmark, R., Zhang, N., Chon, Y., Lin, S.-L., and Klekotka, P. (2012). Mo2083 A randomized, double-blind, placebo-controlled study to evaluate the safety, tolerability, and efficacy of AMG 827 in subjects with moderate to severe crohn's disease. Gastroenterology *143*, e26. https://doi.org/10.1053/j.gastro.2012.07.084.
12. Hueber, W., Sands, B.E., Lewitzky, S., Vandemeulebroecke, M., Reinisch, W., Higgins, P.D.R., Wehkamp, J., Feagan, B.G., Yao, M.D., Karczewski, M., et al. (2012). Secukinumab, a human anti-IL-17A monoclonal antibody, for moderate to severe Crohn's disease: unexpected results of a randomised, double-blindplacebo- controlled trial. Gut *61*, 1693–1700. https://doi.org/10.1136/gutjnl-2011-301668.
13. Cox, J.H., Kljavin, N.M., Ota, N., Leonard, J., Roose-Girma, M., Diehl, L., Ouyang, W., and Ghilardi, N. (2012). Opposing consequences of IL-23 signaling mediated by innate and adaptive cells in chemically induced colitis in mice. Mucosal Immunol. *5*, 99–109. https://doi.org/10.1038/mi.2011.54.
14. Hue, S., Ahern, P., Buonocore, S., Kullberg, M.C., Cua, D.J., McKenzie, B.S., Powrie, F., and Maloy, K.J. (2006). Interleukin-23 drives innate and T cell–mediated intestinal inflammation. J. Exp. Med. *203*, 2473–2483. https://doi.org/10.1084/jem.20061099.
15. Aychek, T., Mildner, A., Yona, S., Kim, K.-W., Lampl, N., Reich-Zeliger, S., Boon, L., Yogev, N., Waisman, A., Cua, D.J., and Jung, S. (2015). IL-23-mediated mononuclear phagocyte crosstalk protects mice from Citrobacter rodentium-induced colon immunopathology. Nat. Commun. *6*, 6525. https://doi.org/10.1038/ncomms7525.
16. Powrie, F., Leach, M.W., Mauze, S., Caddle, L.B., and Coffman, R.L. (1993). Phenotypically distinct subsets of CD4 + T cells induce or protect from chronic intestinal inflammation in C. B-17 scid mice. Int. Immunol. *5*, 1461–1471. https://doi.org/10.1093/intimm/5.11.1461.
17. Miragaia, R.J., Gomes, T., Chomka, A., Jardine, L., Riedel, A., Hegazy, A.N., Whibley, N., Tucci, A., Chen, X., Lindeman, I., et al. (2019). Single-cell transcriptomics of regulatory T cells reveals trajectories of tissue adaptation. Immunity *50*, 493–504.e7. https://doi.org/10.1016/j.immuni.2019.01.001.
18. Burzyn, D., Benoist, C., and Mathis, D. (2013). Regulatory T cells in nonlymphoid tissues. Nat. Immunol. *14*, 1007–1013. https://doi.org/10.1038/ni.2683.
19. Sefik, E., Geva-Zatorsky, N., Oh, S., Konnikova, L., Zemmour, D., McGuire, A.M., Burzyn, D., Ortiz-Lopez, A., Lobera, M., Yang, J., et al. (2015). Individual intestinal symbionts induce a distinct population of RORγ+ regulatory T cells. Science *349*, 993–997. https://doi.org/10.1126/science.aaa9420.
20. Yang, B.H., Hagemann, S., Mamareli, P., Lauer, U., Hoffmann, U., Beckstette, M., Föhse, L., Prinz, I., Pezoldt, J., Suerbaum, S., et al. (2016). Foxp3+ T cells expressing RORγt represent a stable regulatory T-cell effector lineage with enhanced suppressive capacity during intestinal inflammation. Mucosal Immunol. *9*, 444–457. https://doi.org/10.1038/mi.2015.74.
21. Awasthi, A., Riol-Blanco, L., Jäger, A., Korn, T., Pot, C., Galileos, G., Bettelli, E., Kuchroo, V.K., and Oukka, M. (2009). IL-23 receptor GFP reporter mice reveal distinct populations of IL-17-producing cells. J. Immunol. *182*, 5904–5908. https://doi.org/10.4049/jimmunol.0900732.
22. Izcue, A., Hue, S., Buonocore, S., Arancibia-Cárcamo, C.V., Ahern, P.P., Iwakura, Y., Maloy, K.J., and Powrie, F. (2008). Interleukin-23 restrains regulatory T cell activity to drive T cell-dependent colitis. Immunity *28*, 559–570. https://doi.org/10.1016/j.immuni.2008.02.019.
23. Schiering, C., Krausgruber, T., Chomka, A., Fröhlich, A., Adelmann, K., Wohlfert, E.A., Pott, J., Griseri, T., Bollrath, J., Hegazy, A.N., et al.

(2014). The alarmin IL-33 promotes regulatory T-cell function in the intestine. Nature *513*, 564–568. https://doi.org/10.1038/nature13577.

24. Alvarez, F., Istomine, R., Shourian, M., Pavey, N., Al-Aubodah, T.A.F., Qureshi, S., Fritz, J.H., and Piccirillo, C.A. (2019). The alarmins IL-1 and IL-33 differentially regulate the functional specialisation of Foxp3 + regulatory T cells during mucosal inflammation. Mucosal Immunol. *12*, 746–760. https://doi.org/10.1038/s41385-019-0153-5.
25. Cummings, J.H., Pomare, E.W., Branch, W.J., Naylor, C.P., and MacFarlane, G.T. (1987). Short chain fatty acids in human large intestine, portal, hepatic and venous blood. Gut *28*, 1221–1227. https://doi.org/10.1136/gut.28.10.1221.
26. Høverstad, T., and Midtvedt, T. (1986). Short-chain fatty acids in germfree mice and rats. J. Nutr. *116*, 1772–1776. https://doi.org/10.1093/jn/116.9.1772.
27. Smith, P.M., Howitt, M.R., Panikov, N., Michaud, M., Gallini, C.A., Bohlooly-Y, M., Glickman, J.N., and Garrett, W.S. (2013). The microbial metabolites, short-chain fatty acids, regulate colonic Treg cell homeostasis. Science *341*, 569–573. https://doi.org/10.1126/science.1241165.
28. Atarashi, K., Tanoue, T., Shima, T., Imaoka, A., Kuwahara, T., Momose, Y., Cheng, G., Yamasaki, S., Saito, T., Ohba, Y., et al. (2011). Induction of colonic regulatory T cells by indigenous Clostridium species. Science *331*, 337–341. https://doi.org/10.1126/science.1198469.
29. Wiles, S., Pickard, K.M., Peng, K., MacDonald, T.T., and Frankel, G. (2006). In vivo bioluminescence imaging of the murine pathogen Citrobacter rodentium. Infect. Immun. *74*, 5391–5396. https://doi.org/10.1128/IAI.00848-06.
30. Yen, D., Cheung, J., Scheerens, H., Poulet, F., McClanahan, T., Mckenzie, B., Kleinschek, M.A., Owyang, A., Mattson, J., Blumenschein, W., et al. (2006). IL-23 is essential for T cell-mediated colitis and promotes inflammation via IL-17 and IL-6. J. Clin. Invest. *116*, 1310–1316. https://doi.org/10.1172/JCI21404.
31. Morrissey, P.J., Charrier, K., Braddy, S., Liggitt, D., and Watson, J.D. (1993). CD4+ T cells that express high levels of CD45RB induce wasting disease when transferred into congenic severe combined immunodeficient mice. Disease development is prevented by cotransfer of purified CD4+ T cells. J. Exp. Med. *178*, 237–244. https://doi.org/10.1084/jem.178.1.237.
32. Read, S., Malmström, V., and Powrie, F. (2000). Cytotoxic T lymphocyte–associated antigen 4 plays an essential role in the function of Cd25+Cd4+ regulatory cells that control intestinal inflammation. J. Exp. Med. *192*, 295–302. https://doi.org/10.1084/jem.192.2.295.
33. Bouladoux, N., Harrison, O.J., and Belkaid, Y. (2017). The mouse model of infection with Citrobacter rodentium. Curr. Protoc. Im. *119*, 139–148. https://doi.org/10.1002/cpim.34.
34. Li, H., Hsu, H.C., Wu, Q., Yang, P., Li, J., Luo, B., Oukka, M., Steele, C.H., Cua, D.J., Grizzle, W.E., and Mountz, J.D. (2014). IL-23 promotes TCR-mediated negative selection of thymocytes through the upregulation of IL-23 receptor and RORγt. Nat. Commun. *5*, 4259–4313. https://doi.org/10.1038/ncomms5259.
35. Ogasawara, F., Kano, F., Murata, M., Kimura, Y., Kioka, N., and Ueda, K. (2019). Changes in the asymmetric distribution of cholesterol in the plasma membrane influence streptolysin O pore formation. Sci. Rep. *9*, 4548–4610. https://doi.org/10.1038/s41598-019-39973-x.
36. Nagao, K., Tomioka, M., and Ueda, K. (2011). Function and regulation of ABCA1 - membrane meso-domain organization and reorganization. FEBS J. *278*, 3190–3203. https://doi.org/10.1111/j.1742-4658.2011.08170.x.
37. Yokoyama, S. (2006). ABCA1 and biogenesis of HDL. J. Atherosclerosis Thromb. *13*, 1–15. https://doi.org/10.5551/jat.13.1.
38. Rueda, C.M., Rodríguez-Perea, A.L., Moreno-Fernandez, M., Jackson, C.M., Melchior, J.T., Davidson, W.S., and Chougnet, C.A. (2017). High density lipoproteins selectively promote the survival of human regulatory T cells. J. Lipid Res. *58*, 1514–1523. https://doi.org/10.1194/jlr.M072835.
39. Castanho, M.A., Coutinho, A., and Prieto, M.J. (1992). Absorption and fluorescence spectra of polyene antibiotics in the presence of cholesterol. J. Biol. Chem. *267*, 204–209. https://doi.org/10.1016/s0021-9258(18)48480-3.
40. Meng, X., Zhang, K., Li, J., Dong, M., Yang, J., An, G., Qin, W., Gao, F., Zhang, C., and Zhang, Y. (2012). Statins induce the accumulation of regulatory T cells in atherosclerotic plaque. Mol. Med. *18*, 598–605. https://doi.org/10.2119/molmed.2011.00471.
41. Mausner-Fainberg, K., Luboshits, G., Mor, A., Maysel-Auslender, S., Rubinstein, A., Keren, G., and George, J. (2008). The effect of HMG-CoA reductase inhibitors on naturally occurring CD4+CD25+ T cells. Atherosclerosis *197*, 829–839. https://doi.org/10.1016/j.atherosclerosis.2007.07.031.
42. Sorathia, N., Al-Rubaye, H., and Zal, B. (2019). The effect of statins on the functionality of CD4+CD25+FOXP3+ regulatory t-cells in acute coronary syndrome: a systematic review and meta-analysis of randomised controlled trials in Asian Populations. Eur. Cardiol. *14*, 123–129. https://doi.org/10.15420/ecr.2019.9.2.
43. Herold, M., Breuer, J., Hucke, S., Knolle, P., Schwab, N., Wiendl, H., and Klotz, L. (2017). Liver X receptor activation promotes differentiation of regulatory T cells. PLoS One *12*, 01849855–e185013. https://doi.org/10.1371/journal.pone.0184985.
44. Jakobsson, T., Vedin, L.L., Hassan, T., Venteclef, N., Greco, D., D'Amato, M., Treuter, E., Gustafsson, J.Å., and Steffensen, K.R. (2014). The oxysterol receptor LXRβ protects against DSS- and TNBS-induced colitis in mice. Mucosal Immunol. *7*, 1416–1428. https://doi.org/10.1038/mi.2014.31.
45. Flaveny, C.A., Griffett, K., El-Gendy, B.E.D.M., Kazantzis, M., Sengupta, M., Amelio, A.L., Chatterjee, A., Walker, J., Solt, L.A., Kamenecka, T.M., and Burris, T.P. (2015). Broad anti-tumor activity of a small molecule that selectively targets the warburg effect and lipogenesis. Cancer Cell *28*, 42–56. https://doi.org/10.1016/j.ccell.2015.05.007.
46. Schultz, J.R., Tu, H., Luk, A., Repa, J.J., Medina, J.C., Li, L., Schwendner, S., Wang, S., Thoolen, M., Mangelsdorf, D.J., et al. (2000). Role of LXRs in control of lipogenesis. Genes Dev. *14*, 2831–2838. https://doi.org/10.1101/gad.850400.
47. Li, X., and Zheng, Y. (2015). Regulatory T cell identity: formation and maintenance. Trends Immunol. *36*, 344–353. https://doi.org/10.1016/j.it.2015.04.006.
48. Zhou, X., Bailey-Bucktrout, S.L., Jeker, L.T., Penaranda, C., Martínez-Llordella, M., Ashby, M., Nakayama, M., Rosenthal, W., and Bluestone, J.A. (2009). Instability of the transcription factor Foxp3 leads to the generation of pathogenic memory T cells in vivo. Nat. Immunol. *10*, 1000–1007. https://doi.org/10.1038/ni.1774.
49. Rubtsov, Y.P., Niec, R.E., Josefowicz, S., Li, L., Darce, J., Mathis, D., Benoist, C., and Rudensky, A.Y. (2010). Stability of the regulatory T cell lineage in vivo. Science *329*, 1667–1671. https://doi.org/10.1126/science.1191996.
50. Liston, A., and Gray, D.H.D. (2014). Homeostatic control of regulatory T cell diversity. Nat. Rev. Immunol. *14*, 154–165. https://doi.org/10.1038/nri3605.
51. Martin, J.C., Chang, C., Boschetti, G., Ungaro, R., Giri, M., Grout, J.A., Gettler, K., Chuang, L.S., Nayar, S., Greenstein, A.J., et al. (2019). Single-cell analysis of crohn's disease lesions identifies a pathogenic cellular module associated with resistance to anti-TNF therapy. Cell *178*, 1493–1508.e20. https://doi.org/10.1016/j.cell.2019.08.008.
52. Ahern, P.P., Schiering, C., Buonocore, S., McGeachy, M.J., Cua, D.J., Maloy, K.J., and Powrie, F. (2010). Interleukin-23 drives intestinal inflammation through direct activity on T cells. Immunity *33*, 279–288. https://doi.org/10.1016/j.immuni.2010.08.010.
53. Chaudhry, A., Rudra, D., Treuting, P., Samstein, R.M., Liang, Y., Kas, A., and Rudensky, A.Y. (2009). CD4+ regulatory T cells control TH17 responses in a stat3-dependent manner. Science *326*, 986–991. https://doi.org/10.1126/science.1172702.
54. Parham, C., Chirica, M., Timans, J., Vaisberg, E., Travis, M., Cheung, J., Pflanz, S., Zhang, R., Singh, K.P., Vega, F., et al. (2002). A receptor for the heterodimeric cytokine IL-23 is composed of IL-12r 1 and a novel cytokine receptor subunit, IL-23r. J. Immunol. *168*, 5699–5708. https://doi.org/10.4049/jimmunol.168.11.5699.

55. Chaudhry, A., Samstein, R.M., Treuting, P., Liang, Y., Pils, M.C., Heinrich, J.M., Jack, R.S., Wunderlich, F.T., Brüning, J.C., Müller, W., and Rudensky, A.Y. (2011). Interleukin-10 signaling in regulatory T cells is required for suppression of Th17 cell-mediated inflammation. Immunity *34*, 566–578. https://doi.org/10.1016/j.immuni.2011.03.018.

56. Zhou, V., Agle, K., Chen, X., Beres, A., Komorowski, R., Belle, L., Taylor, C., Zhu, F., Haribhai, D., Williams, C.B., et al. (2016). A colitogenic memory CD4+ T cell population mediates gastrointestinal graft-versus-host disease. J. Clin. Invest. *126*, 3541–3555. https://doi.org/10.1172/JCI80874.

57. Krausgruber, T., Schiering, C., Adelmann, K., Harrison, O.J., Chomka, A., Pearson, C., Ahern, P.P., Shale, M., Oukka, M., and Powrie, F. (2016). T-bet is a key modulator of IL-23-driven pathogenic CD4 + T cell responses in the intestine. Nat. Commun. *7*, 11627. https://doi.org/10.1038/ncomms11627.

58. Wang, N., Silver, D.L., Costet, P., and Tall, A.R. (2000). Specific binding of ApoA-I, enhanced cholesterol efflux, and altered plasma membrane morphology in cells expressing ABC1. J. Biol. Chem. *275*, 33053–33058. https://doi.org/10.1074/jbc.M005438200.

59. Timmins, J.M., Lee, J.Y., Boudyguina, E., Kluckman, K.D., Brunham, L.R., Mulya, A., Gebre, A.K., Coutinho, J.M., Colvin, P.L., Smith, T.L., et al. (2005). Targeted inactivation of hepatic Abca1 causes profound hypoalphalipoproteinemia and kidney hypercatabolism of apoA-I. J. Clin. Invest. *115*, 1333–1342. https://doi.org/10.1172/JCI200523915.

60. Wilhelm, A.J., Zabalawi, M., Owen, J.S., Shah, D., Grayson, J.M., Major, A.S., Bhat, S., Gibbs, D.P., Thomas, M.J., and Sorci-Thomas, M.G. (2010). Apolipoprotein A-I modulates regulatory T cells in autoimmune LDLr -/-ApoA-I-/- mice. J. Biol. Chem. *285*, 36158–36169. https://doi.org/10.1074/jbc.M110.134130.

61. Hong, C., Kidani, Y., A-Gonzalez, N., Phung, T., Ito, A., Rong, X., Ericson, K., Mikkola, H., Beaven, S.W., Miller, L.S., et al. (2012). Coordinate regulation of neutrophil homeostasis by liver X receptors in mice. J. Clin. Invest. *122*, 337–347. https://doi.org/10.1172/JCI58393.

62. Valledor, A.F., Hsu, L.C., Ogawa, S., Sawka-Verhelle, D., Karin, M., and Glass, C.K. (2004). Activation of liver X receptors and retinoid X receptors prevents bacterial-induced macrophage apoptosis. Proc. Natl. Acad. Sci. USA *101*, 17813–17818. https://doi.org/10.1073/pnas.0407749101.

63. Hepworth, M.R., Fung, T.C., Masur, S.H., Kelsen, J.R., McConnell, F.M., Dubrot, J., Withers, D.R., Hugues, S., Farrar, M.A., Reith, W., et al. (2015). Group 3 innate lymphoid cells mediate intestinal selection of commensal bacteria-specific CD4+ T cells. Science *348*, 1031–1035. https://doi.org/10.1126/science.aaa4812.

64. Zhou, L., Chu, C., Teng, F., Bessman, N.J., Goc, J., Santosa, E.K., Putzel, G.G., Kabata, H., Kelsen, J.R., Baldassano, R.N., et al. (2019). Innate lymphoid cells support regulatory T cells in the intestine through interleukin-2. Nature *568*, 405–409. https://doi.org/10.1038/s41586-019-1082-x.

65. Aden, K., Rehman, A., Falk-Paulsen, M., Secher, T., Kuiper, J., Tran, F., Pfeuffer, S., Sheibani-Tezerji, R., Breuer, A., Luzius, A., et al. (2016). Epithelial IL-23r signaling licenses protective IL-22 responses in intestinal inflammation. Cell Rep. *16*, 2208–2218. https://doi.org/10.1016/j.celrep.2016.07.054.

66. Rubtsov, Y.P., Rasmussen, J.P., Chi, E.Y., Fontenot, J., Castelli, L., Ye, X., Treuting, P., Siewe, L., Roers, A., Henderson, W.R., et al. (2008). Regulatory T cell-derived interleukin-10 limits inflammation at environmental interfaces. Immunity *28*, 546–558. https://doi.org/10.1016/j.immuni.2008.02.017.

67. Whitfield, J., Littlewood, T., and Soucek, L. (2015). Tamoxifen administration to mice. Cold Spring Harb. Protoc. *2015*, 269–271. https://doi.org/10.1101/pdb.prot077966.

68. Reinoso Webb, C., Den Bakker, H., Koboziev, I., Jones-Hall, Y., Rao Kottapalli, K., Ostanin, D., Furr, K.L., Mu, Q., Luo, X.M., and Grisham, M.B. (2018). Differential susceptibility to T cell-induced colitis in mice: role of the intestinal microbiota. Inflamm. Bowel Dis. *24*, 361–379. https://doi.org/10.1093/ibd/izx014.

69. Barman, M., Unold, D., Shifley, K., Amir, E., Hung, K., Bos, N., and Salzman, N. (2008). Enteric salmonellosis disrupts the microbial ecology of the murine gastrointestinal tract. Infect. Immun. *76*, 907–915. https://doi.org/10.1128/IAI.01432-07.

70. Genzel, L., Rossato, J.I., Jacobse, J., Grieves, R.M., Spooner, P.A., Battaglia, F.P., Fernández, G., Morris, R.G.M., Fernández, G., and Morris, R.G.M. (2017). The yin and yang of memory consolidation: hippocampal and neocortical. PLoS Biol. *15*, 20005311–e2000626. https://doi.org/10.1371/journal.pbio.2000531.

71. Love, M.I., Anders, S., Kim, V., and Huber, W. (2019). RNA-Seq workflow : gene-level exploratory analysis and differential expression [version 1 ; referees : 2 approved]. F1000 Res. *4*, 1070.

72. Comeau, A.M., Douglas, G.M., and Langille, M.G.I. (2017). Microbiome Helper: A Custom and Streamlined Workflow for Microbiome Research. mSystems *2*. https://doi.org/10.1128/mSystems.00127-16.

73. Walters, W., Hyde, E.R., Berg-Lyons, D., Ackermann, G., Humphrey, G., Parada, A., Gilbert, J.A., Jansson, J.K., Caporaso, J.G., Fuhrman, J.A., et al. (2016). Improved bacterial 16S rRNA gene (V4 and V4-5) and fungal internal transcribed spacer marker gene primers for microbial community surveys. mSystems *1*, e00009-15–e00015. https://doi.org/10.1128/mSystems.00009-15.

74. Parada, A.E., Needham, D.M., and Fuhrman, J.A. (2016). Every base matters: assessing small subunit rRNA primers for marine microbiomes with mock communities, time series and global field samples. Environ. Microbiol. *18*, 1403–1414. https://doi.org/10.1111/1462-2920.13023.

75. Martin, M. (2011). Cutadapt removes adapter sequences from high-throughput sequencing reads. EMBnet. j. *17*, 10. https://doi.org/10.14806/ej.17.1.200.

76. Ewels, P., Magnusson, M., Lundin, S., and Käller, M. (2016). MultiQC: summarize analysis results for multiple tools and samples in a single report. Bioinformatics *32*, 3047–3048. https://doi.org/10.1093/bioinformatics/btw354.

77. Caporaso, J.G., Kuczynski, J., Stombaugh, J., Bittinger, K., Bushman, F.D., Costello, E.K., Fierer, N., Peña, A.G., Goodrich, J.K., Gordon, J.I., et al. (2010). QIIME allows analysis of high-throughput community sequencing data. Nat. Methods *7*, 335–336. https://doi.org/10.1038/nmeth.f.303.

78. Callahan, B.J., McMurdie, P.J., Rosen, M.J., Han, A.W., Johnson, A.J.A., and Holmes, S.P. (2016). DADA2: high-resolution sample inference from Illumina amplicon data. Nat. Methods *13*, 581–583. https://doi.org/10.1038/nmeth.3869.

79. Varoquaux, G., Buitinck, L., Louppe, G., Grisel, O., Pedregosa, F., and Mueller, A. (2015). Scikit-learn. GetMobile: Mobile Comp. and Comm. *19*, 29–33. https://doi.org/10.1145/2786984.2786995.

80. Yilmaz, P., Parfrey, L.W., Yarza, P., Gerken, J., Pruesse, E., Quast, C., Schweer, T., Peplies, J., Ludwig, W., and Glöckner, F.O. (2014). The SILVA and "all-species Living Tree Project (LTP)" taxonomic frameworks. Nucleic Acids Res. *42*, 643–648. https://doi.org/10.1093/nar/gkt1209.

81. Quast, C., Pruesse, E., Yilmaz, P., Gerken, J., Schweer, T., Yarza, P., Peplies, J., and Glöckner, F.O. (2013). The SILVA ribosomal RNA gene database project: improved data processing and web-based tools. Nucleic Acids Res. *41*, 590–596. https://doi.org/10.1093/nar/gks1219.

82. Mandal, S., Van Treuren, W., White, R.A., Eggesbø, M., Knight, R., and Peddada, S.D. (2015). Analysis of composition of microbiomes: a novel method for studying microbial composition. Microb. Ecol. Health Dis. *26*, 27663–27667. https://doi.org/10.3402/mehd.v26.27663.

83. Segata, N., Izard, J., Waldron, L., Gevers, D., Miropolsky, L., Garrett, W.S., and Huttenhower, C. (2011). Metagenomic biomarker discovery and explanation. Genome Biol. *12*, R60. https://doi.org/10.1186/gb-2011-12-6-r60.

84. Albaugh, V.L., Banan, B., Antoun, J., Xiong, Y., Guo, Y., Ping, J., Alikhan, M., Clements, B.A., Abumrad, N.N., and Flynn, C.R. (2019). Role of bile acids and GLP-1 in mediating the metabolic improvements of bariatric surgery. Gastroenterology *156*, 1041–1051.e4. https://doi.org/10.1053/j.gastro.2018.11.017.

STAR★METHODS

KEY RESOURCES TABLE

REAGENT or RESOURCE	SOURCE	IDENTIFIER
Antibodies		
Antibodies used for flow cytometry or cell sorting are listed in Supp. Table S2.	N/A	N/A
Bacterial and virus strains		
Citrobacter rodentium (bioluminescent)	Gad Frankel	Wiles, S., Pickard, K.M., Peng, K., MacDonald, T.T., and Frankel, G. (2006). *In vivo* bioluminescence imaging of the murine pathogen Citrobacter rodentium. Infect Immun *74*, 5391–5396. 10.1128/IAI.00848-06.
Critical commercial assays		
Ovation RNA-seq System V2	Tecan, Mannëdorf, Switzerland	N/A
RNAeasy Micro Kit	Qiagen	N/A
Deposited data		
Bulk RNA-seq colonic Treg cells	This paper	GEO: GSE208621
16S sequencing data	This paper	SRA: PRJNA860604
Single-cell RNA-seq ileal Crohn's Disease from Martin et al.	Martin et al.[51]	Martin, J.C., Chang, C., Boschetti, G., Ungaro, R., Giri, M., Grout, J.A., Gettler, K., Chuang, L. shiang, Nayar, S., Greenstein, A.J., et al. (2019). Single-Cell Analysis of Crohn's Disease Lesions Identifies a Pathogenic Cellular Module Associated with Resistance to Anti-TNF Therapy. Cell *178*, 1493–1508.e20. 10.1016/j.cell.2019.08.008.
Experimental models: Organisms/strains		
Rorc^{tdTomato} mouse	This paper	N/A
Il23r$^{flox/flox}$ mouse	Philip Rosenstiel	Aden, K., Rehman, A., Falk-Paulsen, M., Secher, T., Kuiper, J., Tran, F., Pfeuffer, S., Sheibani-Tezerji, R., Breuer, A., Luzius, A., et al. (2016). Epithelial IL-23R Signaling Licenses Protective IL-22 Responses in Intestinal Inflammation. Cell Rep *16*, 2208–2218. 10.1016/j.celrep.2016.07.054.
RT-qPCR primers are in Table S1	N/A	N/A
Software and algorithms		
Prism 9	Graphpad	RRID:SCR_002798
FACSDiva	BD	RRID:SCR_001456
FlowJo	FlowJo	RRID:SCR_008520
Illustrator	Adobe	RRID:SCR_010279
R	r-project.org	RRID SCR_001905
Other		
Code for reanalysis of single-cell RNA-seq ileal Crohn's Disease	This paper	https://github.com/Ken-Lau-Lab/IL23Ranalysis
Code for analysis of bulk RNA-seq data and 16S	This paper	Data S1

RESOURCE AVAILABILITY

Lead contact

Further information and requests for resources and reagents should be directed to and will be fulfilled by the lead contact, Jeremy Goettel (jeremy.goettel@vumc.org).

Materials availability

Rorc^{tdTomato} reporter mice are available from the lead contact upon request.

Data and code availability

- Code for analysis of bulk RNA-seq and 16S is included as Data S1 Code for analysis of bulk RNA-seq data and 16S, related to Figures S4 and 4, and data have been deposited at GEO and SRA respectively and are publicly available as of the date of publication. Accession numbers are listed in the key resources table. This paper re-analyzes existing publicly available data from Martin et al.[51].
- Original single-cell RNA-seq code is available at GitHub and is publicly available as of the data of publication. A link is listed in the key resources table. Original bulk RNA-seq code will be shared by the lead contact upon request.
- Any additional information required to reanalyze the data reported in this paper is available from the lead contact upon request.

EXPERIMENTAL MODEL AND SUBJECT DETAILS

Mice

Mice lacking the IL-23R specifically in Treg cells were generated by crossing *Il23r*$^{flox/flox}$ mice[65] with *Foxp3*$^{YFP\text{-}Cre}$ mice[66] (The Jackson Laboratory, Bar Harbor, ME, stock #016959) (*Il23r*$^{\Delta Treg}$ mice). The LoxP sites flank exon 4 of *Il23r*, which encodes for the extracellular domain of IL-23R.[65] To validate successful excision of the floxed alleles in Treg cells specifically, enrichment for $CD4^+$ or $CD4^+CD25^+$ was performed followed by cell sorting of live $CD4^+CD25^+YFP^+$ cells. DNA was then extracted using the DNeasy Blood & Tissue kit (Qiagen, Germantown, MD), followed by PCR (forward 5′-TCAAAGTTGACTACACTGTAAGGTAGAGGTAGTGG and reverse primer 5′-GGTGGATCTGCAACAAAACGAATCAC). *Il23r*$^{flox/flox}$ mice were also crossed with mice expressing a Cre recombinase under a *Cd2* (JAX stock #008520) or *Vav* (JAX stock #008610) promoter to delete IL-23R specifically in lymphocytes or all hematopoietic cells, respectively. To enable lineage tracing, *ROSA26*$^{lox\text{-}stop\text{-}lox\text{-}tdTomato}$ (JAX stock #007914) mice were crossed with *Foxp3*$^{EGFP-Cre-ERT-2}$ mice (JAX stock #016961) to obtain *Rosa26*$^{lox\text{-}stop\text{-}lox\text{-}tdTomato}$;*Foxp3*$^{eGFP-Cre-ERT2}$ mice. Mice were administered 8 mg tamoxifen (Sigma-Aldrich, St. Louis, MO) in 200 μL olive oil (Sigma-Aldrich) by oral gavage on day 0, 1, and 3.[49,67] Mice were housed in a specific-pathogen free vivarium at Vanderbilt University Medical Center (VUMC). *Rag1*$^{-/-}$ mice (JAX stock #002216) were housed in sterilized cages and provided autoclaved food and water. Experiments with *Citrobacter rodentium*[29] were performed in an ABSL2 facility. Homozygous *Il23r*^{eGFP} mice (JAX stock #035863) were used to examine IL-23R expression by flow cytometry. All experiments were performed using 6–8-week-old female or male mice unless otherwise indicated. Littermates were used where possible, which, due to the multiple genetic alterations could not always be accomplished. Mice were co-housed and bedding mixed to equalize the intestinal microbiome as much as possible. Experiments were approved by the VUMC Institutional Animal Care and Use Committee.

METHOD DETAILS

Colonic lamina propria

Colons were removed, opened longitudinally, washed with cold PBS, cut into 5 mm pieces, and incubated in 50-mL conical tubes containing 25 mL pre-warmed RPMI 1640 media with 5% FBS, 5 mM EDTA, 1 mM dithiothreitol (Thermo Fisher), and 20 mM HEPES at 37°C for 40 minutes in a non-CO_2 MaxQ4450 horizontal shaker (Thermo Fisher Scientific, Waltham MA). The media was then strained through a sieve (Everyday Living, available from Kroger, Nashville, TN), and intestinal pieces were placed into 25 mL cold RPMI 1640 media containing 2 mM EDTA, and 20 mM HEPES, shaken vigorously 20 times, and strained again. Intestinal pieces were then minced and placed into 25 mL prewarmed RPMI 1640 media containing 0.1 $mgml^{-1}$ Liberase TL (Roche, Basel, Switzerland), 0.05% DNAse I (Sigma-Aldrich, D5025) and 20 mM HEPES and shaken at 37°C for 30 minutes. Cells were pulled through a 10 mL syringe 20 times and filtered through a 70 μm cell strainer into an equal volume of cold RPMI 1640 media containing 5% FBS, 0.05% DNAse I, 20 mM HEPES on ice. Cells were spun for 10 minutes at 4°C and 475 × g and resuspended in 40% Percoll (Sigma-Aldrich) solution and underlaid using 90% Percoll. The 40/90 gradient was spun for 25 minutes at 20°C at 475 × g with no brake or acceleration applied. The interphase layer was recovered and washed in fluorescence activated cell sorting (FACS) buffer (PBS with 2% FBS and 2 mm EDTA) and spun again for 10 minutes at 20°C and 475 × g prior to downstream application(s).

Adoptive transfer colitis and *in vivo* Treg cell induction

Naïve T cells were sorted based on live $CD4^+CD25^-YFP^-CD45RB^{hi}$ expression following pre-enrichment for $CD4^+$ cells using negative selection (#19852 from Stem Cell Technologies, Vancouver, Canada). For Treg cell and naïve $CD4^+$ T cell transfer experiments, *Rag1*$^{-/-}$ mice were injected via intraperitoneal route with 5×10^5 naïve T cells[16] with or without IL-23R-sufficient or IL-23R-deficient Treg cells in a single injection of 200 μL PBS at ratios of 20:1 to naïve:Treg cells. As colitis in the adoptive transfer model is dependent on a complex microbiota containing *Helicobacter spp.*, bedding from mice housed in non-autoclaved cages was mixed into the cages of recipient mice at the time of injection and mice were removed from sterile housing conditions.[68] Mice were monitored weekly for colitis using weight loss as a clinical parameter. All mice were expected to develop colitis even those co-injected a limited number of Treg cells. In rare cases, mice that failed engraftment/expansion of naïve T cells as assessed by the frequency of splenic $CD4^+CD3^+$ T cells were excluded from histological analysis.

In vitro Treg cell suppression

Naïve T cells from spleen and mLN were enriched from *Il23r*$^{flox/flox}$;*Cd2*^{Cre} mice (lacking IL-23R in all lymphocytes) using a naïve T cell isolation kit (Stem Cell Technologies) and labeled with CellTrace Violet (Thermo Fisher Scientific) according to manufacturer's protocol. Cells were counted and stimulation was performed using αCD3αCD28 Dynabeads (Thermo Fisher). Cells were cultured for 72 hours together with 10,000 FACS-sorted WT colonic YFP^+ Treg cells in a 1:1 Treg:Tnaïve ratio in the presence or absence of 20 $ngmL^{-1}$ recombinant mIL-23 or IL-6 (R&D Systems). Proliferation was assessed via CellTrace Violet dilution in naïve T cells and % suppression determined.

Histology

Hematoxylin and eosin (H&E) staining was performed by the Vanderbilt Translational Pathology Shared Resource on formalin-fixed paraffin-embedded (FFPE) colon sections. Scoring of histology was performed by pathologist (MKW) who was blinded to genotype and treatment condition.

In vitro Treg cell induction

Treg cells were induced *in vitro* by coating a flat bottom 48-well plate with 5 μgml^{-1} αCD3 overnight at 4°C. The plate was washed twice with cold PBS and 2×10^5 naive $CD4^+$ cells were incubated for 96 hours in TCM containing 1 μgml^{-1} αCD28 (Thermo Fisher), 2 $ngml^{-1}$ human TGFβ1 (R&D systems, Minneapolis, MN) 1 μgml^{-1} anti-IFNγ (BD), and 1 μgml^{-1} anti-IL-4 (BD).

Mixed bone marrow chimeras

Rag1$^{-/-}$ recipient mice were pre-conditioned with 450 rads of ^{137}Cs source radiation. Conditioned mice were retro-orbitally injected with 5×10^6 congenically-marked lineage-depleted (ThermoFisher Scientific) bone marrow cells recovered from the tibiae and femurs of $CD45.1^+$;*Foxp3*$^{YFP-Cre}$ mice and $CD45.2^+$;*Il23r*$^{\Delta Treg}$ mice in a 1:1 ratio. Recipient mice received 0.4 $mgml^{-1}$ enrofloxacin (Baytril, Bayer, KS) in the drinking water 4 days pre-to 7 days post-transplant. Lineage depletion was confirmed by flow cytometry and screening for engraftment was performed 6–8 weeks post-reconstitution.

Liver X receptor

SR9243 (Cayman Chemicals) was used an inverse agonist for LXR. Mice were injected with 30 $mgkg^{-1}$ daily for 5 days with euthanasia on day 6. T0901317 (Cayman Chemicals) was used as an agonist for LXR at a final concentration of 10 uM. For all *in vitro* Treg cell cultures without naïve T cells, Treg cells were stimulated with αCD3αCD28 Dynabeads in round-bottom plates supplemented with 30 IU/mL recombinant IL-2 (Biolegend). Compounds were purged with nitrogen where indicated by the manufacturer.

Antibiotic treatment

Mice were given antibiotics in the drinking water as described by Atarashi et al.[28] Opaque water bottles were implemented, and fresh water was prepared at weekly. Concentration of antibiotics used: vancomycin 500 mg, ampicillin 500 mg, neomycin 1 g, metronidazole 1 g all per 1 L. Universal 16S primers were used to confirm reduction of bacteria after antibiotic treatment using a protocol previously described.[69]

RNA isolation

RNA extraction from cells was performed using the RNeasy Mini Kit (Qiagen). For low cell numbers the RNAeasy Micro Kit (Qiagen) was used, and cells were sorted directly into 300 μL RLT buffer containing 2-mercapto-ethanol as recommended. Extraction of RNA from whole tissue was performed on tissue stored in RNA-later (Sigma-Aldrich) until homogenization using a Tissue-Tearor (Dremel, Racine, WI), followed by phenol/chloroform extraction as described[70] or extraction using a combination of phenol/chloroform extraction and the RNeasy Mini Kit. On column DNAse treatment was performed as per manufacturer's recommendations.

Quantitative RT-PCR (qRT-PCR)

First strand cDNA synthesis was performed using SuperScript VILO IV MasterMix (Thermo Fisher Scientific). qRT-PCR was performed using PowerUp SYBR green (Sigma-Aldrich) on a QuantStudio3 or Quantstudio 6 (Thermo Fisher Scientific). Relative expression was quantified using the delta-delta Ct method with genes of interest referenced to *Tbp*. Primers are in Table S1.

RNA-sequencing

Quality control for RNA was performed by the Vanderbilt Technologies for Advanced Genomics core using RNA 6000 Pico (Agilent, Santa Clara CA), and for low-input RNA from colonic Treg cells followed by RNA amplification using Ovation RNA-seq System V2 (Tecan, Mannëdorf, Switzerland), and cDNA library preparation using a NEB library preparation kit. Paired end 150bp sequencing was performed on a NovaSeq 6000 (Illumina, San Diego, CA). Samples were trimmed with fastp (version 0.20.0) using default parameters. Quantification was performed using Salmon (version 1.4.0) against a decoy transcriptome (Mus musculus Gencode version 21 or Homo sapiens Gencode version 29). Further analysis was performed in R (version 4.1.2) in R studio (version 2021.09.2 + 382) based on a pipeline described by Love et al.[71] Briefly, quantification files were imported with tximeta (version 1.2.2) and genes with counts ≤ 1 were omitted. Normalization was performed for principal component analysis and gene clustering plots with variance stabilizing transformation and regularized-logarithm transformation, respectively. Differential expression analysis was performed on non-normalized counts using DESEq2 (version 1.34.0). For analysis with more than two groups, limma (version 3.50.3) was used on log-CPM transformed counts with prior count = 3. Annotation was done with AnnotationDbi (version 1.56.2) using org.Hs.eg.db (version 3.14.0) or org.Mm.eg.db (version 3.14.0). Images were generated with pheatmap (version 1.0.12), RColorBrewer (version 1.1-3), ggplot2 (version 3.3.5), and EnhancedVolcano (version 1.12.0).

16S sequencing

Fresh stool pellets were collected from live mice, flash-frozen and stored at −80°C until DNA extraction. DNA was extracted using the QIAmp PowerFecal DNA kit (Qiagen). 16S library preparation and 16S sequencing was performed by the Integrated Microbiome Resource at Dalhousie University in Canada.[72] Sequencing was performed for V4-V5 on an Illumina MiSeq, (300bp PE). Reads (Primer forward GTGYCAGCMGCCGCGGTAA, primer reverse CCGYCAATTYMTTTRAGTTT[73,74]) were trimmed using Cutadapt[75] and untrimmed reads were discarded. Quality control results were summarized with MultiQC[76] and trimmed reads loaded in QIIME version 2 2019.4.[77] Further quality control was done in QIIME by trimming reads based on the sample position where the quality dropped below a quality score of 30 using the dada2 plugin.[78] Rarefaction was performed to ensure even sampling with sequences classified for taxonomic analysis by training a Naive Bayes classifier[79] using the SILVA reference taxonomy dataset[80,81] (release 132, 16S only, 99%, majority taxonomy all levels, primer sequences as above). Differential abundance was tested with the ANCOM plugin,[82] which assumes less then 25% of features are different between conditions. Preceding differential abundance testing, taxa were collapsed to the appropriate levels. Features that were detected less than 10 times in total or features detected in only one sample were excluded from analysis. A pseudo count of 1 was added to enable log transformation required for ANCOM. LDA Effect Size (LEfSe) was performed using Galaxy developed by the Huttenhower group.[83]

Flow cytometry

For cell surface staining, cells were incubated in the antibody cocktail for 20 minutes at 4°C in the dark. Samples were blocked using 30 μL normal rat serum (StemCell Technologies). Intracellular cytokine staining was performed using Cytofix/Cytoperm (BD) and intranuclear stain was performed using the FOXP3 staining buffer set (eBioscience, San Diego, California), both according to manufacturer's instructions. Filipin-III was stained after overnight fixation of cells. Annexin-V staining was performed following the manufacturers' instructions (ThermoFisher Scientific) by staining for 15 minutes at room temperature using Ca^{2+}-containing Annexin-V buffer (diluted from 5X stock to 1X with ultrapure water). Cells were washed in room temperature also using Annexin V buffer prior to analysis. Flow cytometric analysis was performed using a 4-Laser Fortessa or 5-laser LSRII (BD) with FACSDiva software (BD). Fluorescence-activated cell sorting (FACS) was performed on a FACS Aria III (BD). Analyses were performed using FlowJo (BD Biosciences). For all flow experiments, a live/dead stain (ThermoFisher) was used to only assess live cells. Antibodies used for flow cytometry or cell sorting are listed in Table S2.

Bile acid analysis

Bile acids were profiled by LC-ESI-MS/MS as recently described.[84] Briefly, to 50 μL of serum was added 200 μL of 100 mM aqueous sodium hydroxide or to 50 mg feces was added 500 and 50 μL of 100 mM aqueous sodium hydroxide of a 2 nM internal standard mix of deuterium-labeled bile acids including d4-labeled chenodeoxycholic acid (d4-CDCA), taurocholic acid (d4-TCA), glycochenodeoxycholic acid (d4-GCDCA), cholic acid (d4-CA), glycocholic acid (d4-GCA) (all purchased from C.D.N. Isotopes Inc., Point Claire, Montreal, PQ, Canada) and tauro-beta-muricholic acid (d4-TβMCA) (US Biological Corp., Swampscott, MA). Samples were heated at 64°C for 30 minutes, centrifuged for 10 minutes at 14,400*g*, and the supernatant acidified to pH 7.0 with 50 μL of 0.1M hydrochloric acid. The sample was brought to a final volume of 1 mL with water and applied to a 1-mL (30 mg) Oasis HLB cartridge (Waters, Milford, MA) previously equilibrated first with 1 mL methanol, then 1 mL water. The column-bound bile acids were washed with 1 mL 5% (vol/vol) aqueous methanol, then 1 mL 2% (vol/vol) aqueous formic acid. Bile acids were eluted from the column with 1 mL 2% (vol/vol) ammonia in methanol and the eluent evaporated to dryness using a rotary evaporator at 30°C for 2 hours. Samples were

resuspended in 100 μL 25% (vol/vol) acetonitrile in water. An Acquity UPLC system (Waters, Milford, MA) was used with an Acquity UPLC BEH C18 1.7-μm, 2.1 × 150-mm column (Waters), and heated to 50°C, and a binary solvent system of 10% (vol/vol) acetonitrile in water (mobile phase A) and 90% (vol/vol) acetonitrile in water (mobile phase B), both containing 20 mM ammonium acetate was used to resolve plasma bile acids. Mass spectrometry analysis was performed using a TSQ Quantum mass spectrometer (ThermoFinnigan) equipped with an ESI probe in negative-ion mode. The following (optimized) parameters were used for the detection of the analytes and the internal standard: N2 sheath gas, 49 psi; N2 auxiliary gas, 25 psi; spray voltage, 3.0 kV; source CID, 25 V; capillary temperature, 300°C; capillary offset, −35 V; tube lens voltage, 160 V; Q2 gas pressure, 1.5 mtor; Q3 scan width 1 m/z; Q1/Q3 peak widths at half-maximum, 0.7 m/z. Stock solutions of 2.5 mM of all bile acids (CA, CDCA, DCA, HDCA, UDCA, TCA, TCDCA, TDCA, TLCA, THCA, TUDCA, THCA, HCA, αMCA, βMCA, TαMCA, TβMCA, TωMCA, THDCA) were used to prepare calibrators with concentrations of 100 μM in methanol. After preparation of calibrators, bile acids were mixed to achieve final concentrations of 50, 20, 2.5, 0.75, 0.25, 0.05, 0.015, and 0.005 μM. Calibration curves and concentration of individual bile acids were calculated by LCQuan 2.5.5 software (ThermoFinnigan). Concentrations of individual bile acids were calculated from peak area in the chromatogram detected with SRM relative to the appropriate internal standard.

QUANTIFICATION AND STATISTICAL ANALYSIS

Details regarding the statistical analyses are indicated in the figure legends. *N* represents biological replicates, and where indicated one replicate (datapoint) can consist of data from multiple mice. Data shown are representative or pooled data from at least two independent experiments with similar results. RNA-sequencing (RNA-seq) and 16S sequencing experiments were performed for multiple samples. The sequence of sample processing was counterbalanced. Age-, gender- and, where feasible, littermate-matched mice were used. Apart from 16S and bulk RNA-seq, statistical analyses were performed using GraphPad Prism (9.1.2). Sample size was determined empirically.

Cell Reports, Volume *42*

Supplemental information

Interleukin-23 receptor signaling impairs the stability and function of colonic regulatory T cells

Justin Jacobse, Rachel E. Brown, Jing Li, Jennifer M. Pilat, Ly Pham, Sarah P. Short, Christopher T. Peek, Andrea Rolong, M. Kay Washington, Ruben Martinez-Barricarte, Mariana X. Byndloss, Catherine Shelton, Janet G. Markle, Yvonne L. Latour, Margaret M. Allaman, James E. Cassat, Keith T. Wilson, Yash A. Choksi, Christopher S. Williams, Ken S. Lau, Charles R. Flynn, Jean-Laurent Casanova, Edmond H.H.M. Rings, Janneke N. Samsom, and Jeremy A. Goettel

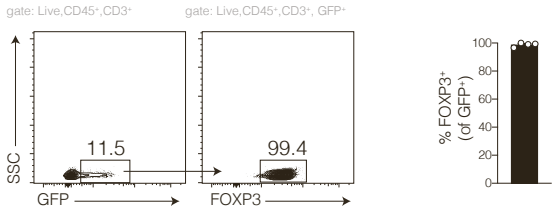

Figure S1: *Foxp3*$^{YFP\text{-}Cre}$ mice faithfully mark FOXP3^{+} cells. Related to figure 1.
Representative gating and Treg cell frequency by GFP and FOXP3 co-stain of paired samples from co-housed *Foxp3*$^{YFP\text{-}Cre}$ mice and wild type C57BL/6 mice. The GFP antibody is cross-reactive for YFP.

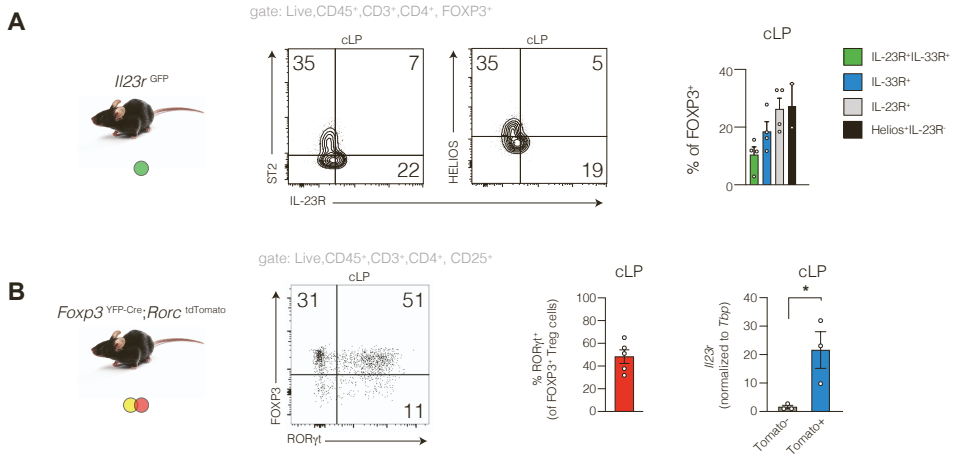

Figure S2: IL-23R is predominantly co-expressed with RORγt but not IL-33R on colonic Treg cells. Related to figure 1.

(A) Representative gating and Treg cell phenotype of colonic Treg cells in *Il23r*^{eGFP} mice. (B) RORγt^{+} and RORγt^{neg} cells were quantified (in three independent experiments) and flow-sorted (in two independent experiments) from *Foxp3*$^{YFP\text{-}Cre}$*Rorc*^{tdTomato} reporter mice followed by RT-qPCR (right). Unpaired t-test. * $p < 0.05$.

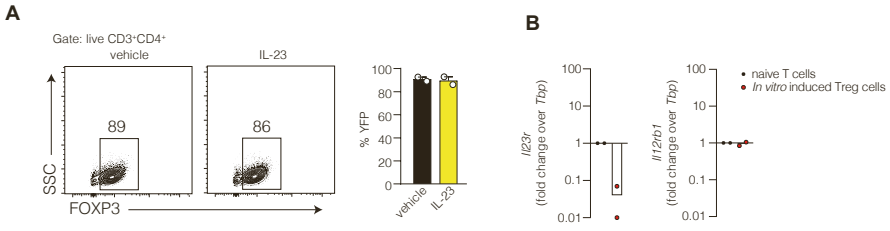

Figure S3: IL-23 does not inhibit Treg cell induction *in vitro.* Related to figure 1.
(A) YFP^{-} naïve T cells from *Foxp3*$^{YFP\text{-}Cre}$ mice were enriched via negative selection and differentiated *in vitro* into Treg cells in the presence or absence of IL-23 for four days. Gating strategy and quantification of YFP^{+} cells as a percentage of live cells. (B) Representative qRT-PCR analysis of FACS-sorted YFP^{+} Treg cells induced *in vitro* compared to naïve T cells.

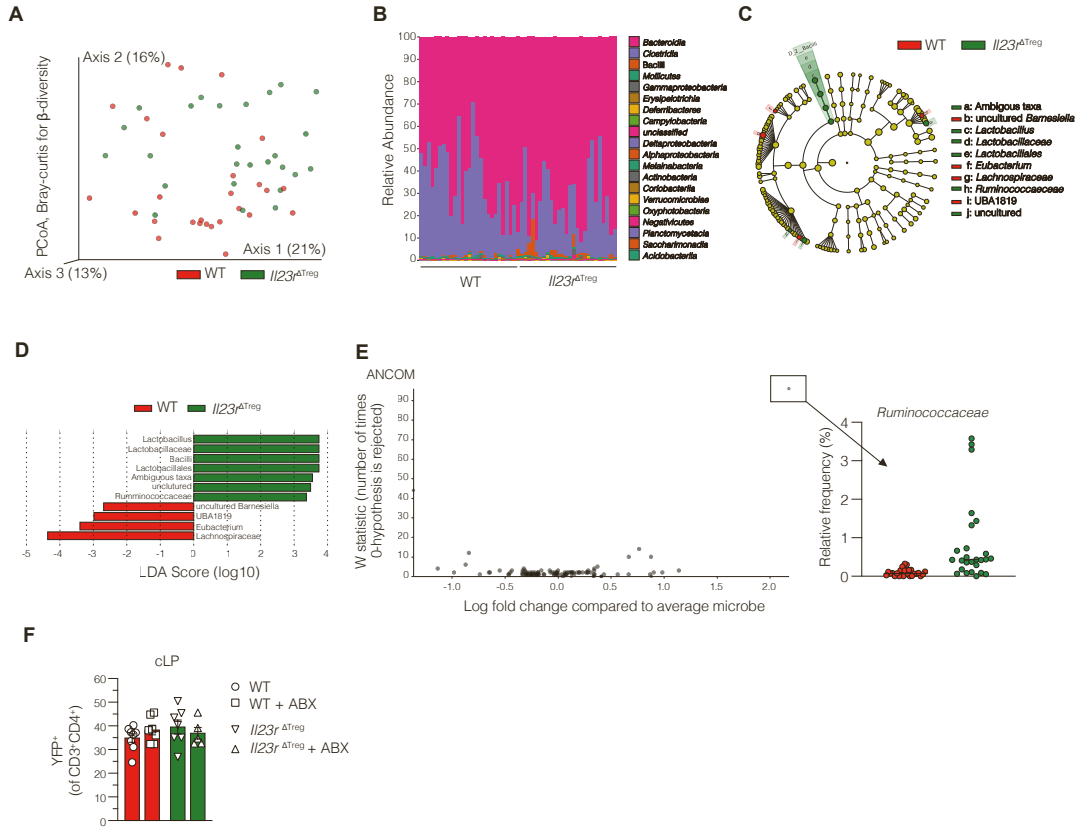

Figure S4: The intestinal microbiome of *Il23r*$^{\Delta Treg}$ mice is not significantly altered compared to *Foxp3*$^{YFP\text{-}Cre}$ mice. Related to figure 1.

16S sequencing was performed on fresh stool recovered from independently housed *Foxp3*$^{YFP\text{-}Cre}$ and *Il23r*$^{\Delta Treg}$ mice. (A) Principal coordinates analysis (Bray-curtis for β diversity). (B) Bar plot of bacteria taxa. (C) Cladogram depicting enriched bacteria between groups. (D) Linear discriminant analysis (LDA) scores between groups. (E) ANCOM identifying significantly increased *Ruminococceae* in *Il23r*$^{\Delta Treg}$ mice (left) with relative frequency (right). (F) Mice were treated with broad-spectrum antibiotics for 3 months with Treg cells were quantified in the colon at experiment endpoint.

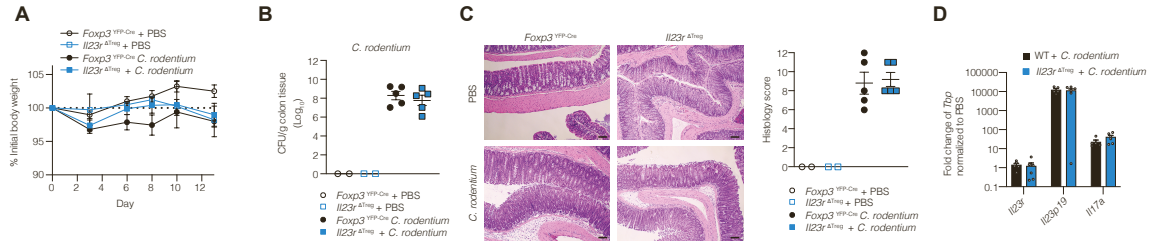

Figure S5: Treg cell-specific IL-23R deficiency does not alter susceptibility to *C. rodentium*-induced colitis. Related to figure 2.

(A) Mouse body weight calculated against initial weight over the course of experiment. (B) Quantification of *C. rodentium* CFU at experimental endpoint. (C) H&E-stained colon sections showing representative histology (left) and quantified (right). (D) Th17 related gene expression in affected colon tissue. (B, C, D) t-test within the mice exposed to *C. rodentium*. Histogram bars represent the mean ± SEM. Data are representative of two independent experiments.

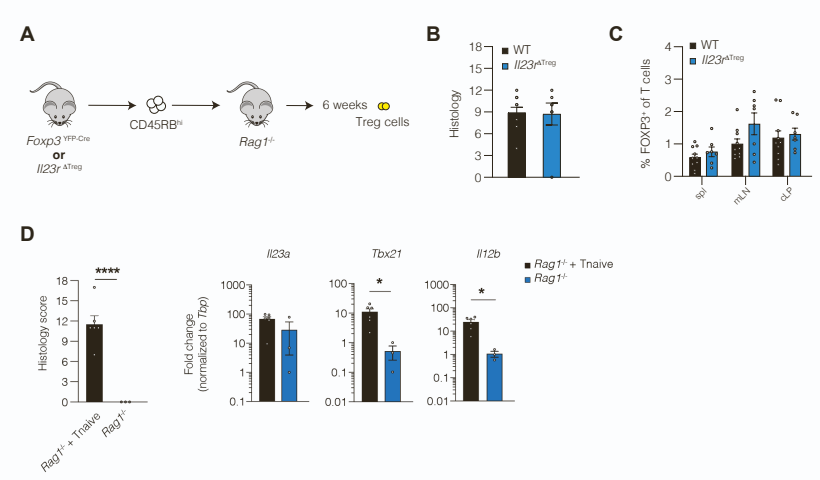

Figure S6: Survival/expansion of post-converted Treg cells is not altered by IL-23R deficiency in a transfer setting. Related to figure 2. Naïve T cells ($CD45^{+}CD3^{+}CD4^{+}CD25^{-}CD45RB^{hi}$) were sorted from WT and *Il23r*$^{\Delta Treg}$ mice injected into *Rag1*$^{-/-}$ recipients and assessed YFP^{+} cells 6 weeks later. (B) Histologic injury score and (C) Treg cell frequency at 6 weeks after injection. (D) Histological scoring and qPCR of colonic tissue at 6 weeks following the transfer of naive T cells sorted from WT mice into *Rag1*$^{-/-}$ mice.

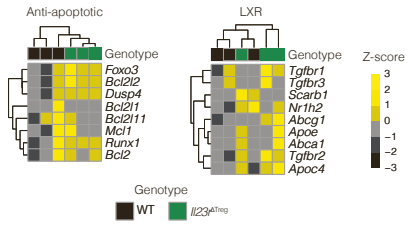

Figure S7: IL-23R-deficient colonic Treg cells exhibit alterations in genes associated with LXR signaling and cell survival. Related to figure 4. RNA-sequencing was performed on FACS-sorted Treg cells ($CD4^+CD45^+FOXP3^+$ cells) from the cLP of *Foxp3*$^{YFP\text{-}Cre}$ and *Il23r*$^{\Delta Treg}$ mice (see also Figure 4). Heatmaps with Z-scores of genes of interest pertaining to apoptosis of Treg cells (left) and LXR signaling (right). Each sample (column) is representative of at least 5 mice.

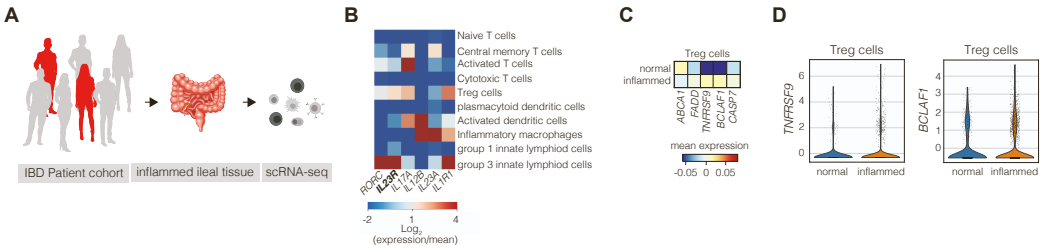

Figure S8: IL-23 alters genes associated with regulating LXR signaling and apoptosis in human cells. Related to figure 5. (A) Schematic of single-cell RNA-seq dataset[51]. (B) *IL23R* expression in Crohn's disease from inflamed ileum. (C-D) Supervised analysis of the Treg cell focused cluster in the same dataset comparing Treg cells recovered from non-inflamed region vs inflamed lesions.

Table S1 RT-qPCR primers

Target	Species	Sequence	Primer bank ID
mIl23r F	Mouse	GCTCGGATTTGGTATAAAGG	NA
mIl23r R	Mouse	ACTTGGTATCTATGTAGGTAGG	
mIl23 F	Mouse	CTGCTTGACTCTGACATC	NA
mIl23 R	Mouse	CACTGCTGACTAGAACTC	
mIl12rb1 F	Mouse	ACTGGAATGTGTCTGAAG	NA
mIl12rb1 R	Mouse	CGTATCTGGATCTCTTGG	
mIL-17A F	Mouse	TTTAACTCCCTTGGCGCAAAA	6754324a1
mIL-17A R	Mouse	CTTTCCCTCCGCATTGACAC	
mRorc F	Mouse	GACCCACACCTCACAAATTGA	6755344a1
mRorc R	Mouse	AGTAGGCCACATTACACTGCT	
mFoxp3 F	Mouse	CCCATCCCCAGGAGTCTTG	16905075a1
mFoxp3 R	Mouse	ACCATGACTAGGGGCACTGTA	
mTbx21 F	Mouse	AGCAAGGACGGCGAATGTT	9507179a1
mTbx21 R	Mouse	GGGTGGACATATAAGCGGTTC	
mIl12b F	Mouse	TGGTTTGCCATCGTTTTGCTG	6680397a1
mIl12b R	Mouse	ACAGGTGAGGTTCACTGTTTCT	
mIFNg F	Mouse	ATGAACGCTACACACTGCATC	33468859a1
mIFNg R	Mouse	CCATCCTTTTGCCAGTTCCTC	
mTGFb1 F	Mouse	CTCCCGTGGCTTCTAGTGC	6755775a1
mTGFb1 R	Mouse	GCCTTAGTTTGGACAGGATCTG	
mTGFb2 F	Mouse	CTTCGACGTGACAGACGCT	15029686a1
mTGFb2 R	Mouse	GCAGGGGCAGTGTAAACTTATT	
mTBP F	Mouse	CTTCCTGCCACAATGTCACAG	10181156a1
mTBP R	Mouse	CCTTTCTCATGCTTGCTTCTCTG	
mRegIIIg Fw	Mouse	CCATCTTCACGTAGCAGC	NA
mRegIIIg Rv	Mouse	CAAGATGTCCTGAGGGC	
mIL-6 f	Mouse	TAGTCCTTCCTACCCCAATTTCC	13624311a1
mIL-6 r	Mouse	TTGGTCCTTAGCCACTCCTTC	
mIL-1 f	Mouse	GCAACTGTTCCTGAACTCAACT	6680415a1
mIL-1 r	Mouse	ATCTTTTGGGGTCCGTCAACT	
mTGFbr1 f	Mouse	TCTGCATTGCACTTATGCTGA	12853637a1
mTGFbr1 r	Mouse	AAAGGGCGATCTAGTGATGGA	
mTGFbr2 f	Mouse	CCGCTGCATATCGTCCTGTG	27363474a1
mTGFbr2 r	Mouse	AGTGGATGGATGGTCCTATTACA	
mTGFbr3 f	Mouse	GGTGTGAACTGTCACCGATCA	33469109a1
mTGFbr3 r	Mouse	GTTTAGGATGTGAACCTCCCTTG	
mTGFbr1v2 f	Mouse	CAGCTCCTCATCGTGTTGGTG	483376a1
mTGFbr1v2 r	Mouse	GCACATACAAATGGCCTGTCTC	

For RT-qPCR on human samples Taqman probes were used. m: mouse.

Related to STAR methods

Table S2 FACS antibodies

Antigen-label	Source	Cat#; Identifier
CD25-BV421	Biolegend	102034; RRID:AB_11203373
CD4-APC-Cy7	Biolegend	100414; RRID:AB_312699
CD62L-BV605	Biolegend	104437; RRID:AB_11125577
CD45-BV785	Biolegend	103149; RRID:AB_2564590
CD45RB-BV711	BD Bioscience	740654; RRID:AB_2740343
CD3-PE-Cy7	Biolegend	100320; RRID:AB_312685
CD44-PE-Cy5	Biolegend	103010; RRID:AB_312961
FOXP3-PerCP/Cy5.5	eBioscience	45-5773-82
GFP-Alexa fluor 647	Biolegend	338005; RRID:AB_1279413
CD4-FITC	Biolegend	116003; RRID:AB_313688
CD45.2-BV421	Biolegend	109832; RRID:AB_2565511
IL-4-PerCP/Cy5.5	Biolegend	504123; RRID:AB_2561564
IFNgamma-APC	Biolegend	505810; RRID:AB_315404
IL-17A-BV421	Biolegend	506926; RRID:AB_2632611
CD8-PerCP/Cy5.5	Biolegend	126609; RRID:AB_961304
Annexin-V-PE	Invitrogen	A35111
CD45.1-BV711	Biolegend	110739; RRID:AB_2562605
CD25-APC	eBioscience	17-0390-82
Rorgt-PE-eFluor610	eBioscience	61-6981-82
CD44-BV785	Biolegend	103041; RRID:AB_11218802
CD44-APC	Biolegend	103012; RRID:AB_312963
Annexin-V APC	Tonbo	20-6409-T100
Fillipin-III	Cayman Chemical	70440
Ki67-eFluor450	Thermofisher	48-5698-80
GFP-PE-Cy7	Biolegend	338013; RRID:AB_2860869
Rorgt-BV421	BD Bioscience	562894; RRID:AB_2687545
ST2-APC	Biolegend	146605; RRID:AB_2728174
CD45-SparkYG570	Biolegend	103171; RRID:AB_2832303
CD4-APCFire810	Biolegend	100480
HELIOS-AF700	Biolegend	137241; RRID:AB_2832496

Relates to STAR methods